

Author's response to reviews of "A nondimensional framework for exploring the relief structure of landscapes" by S. W. D. Grieve et al.

Stuart W. D. Grieve¹, Simon M. Mudd¹, Martin D. Hurst², and David T. Milodowski¹

¹School of GeoSciences, University of Edinburgh, Drummond Street, Edinburgh EH8 9XP, UK

²British Geological Survey, Keyworth, Nottingham NG12 5GG, UK

Correspondence to: Stuart W. D. Grieve (s.grieve@ed.ac.uk)

In this document, reviewers comments are presented in **bold type** and our responses are in standard type. Following our responses to the review comments, a copy of the manuscript with our changes highlighted is included.

5 Review 1

Grieve et al. propose a framework for computing the dimensionless relief and erosion rates of ridge-and-valley topography using a combination of valley network extraction and hilltop curvature analysis. They argue that their approach allows one to determine whether or not a landscape is in topographic steady state and to determine the mean Sc value (the maximum
10 gradient of stability) of a landscape. Overall I think the paper will be an excellent contribution, once some issues are thoroughly considered and/or caveats provided.

We would firstly like to thank the reviewer for their positive and thorough appraisal of our work. We are pleased that the reviewer considers the manuscript and accompanying software to be worth-
15 while and believe that through this discussion the manuscript has been significantly improved. We have added additional discussion into the manuscript to account for the limitations highlighted by the reviewer, have enhanced the theoretical background to place the work in a better context and have added additional detail to the methodology to clarify how our data is extracted. We respond to each point made by the reviewer individually below.

20

(1) I am skeptical that the mean value of Sc is 0.79 in the Oregon Coast Range. Roering et al. (1999) demonstrated that many hillslopes in the OCR have gradients in the 0.8 to 1.1 range, and more importantly that the planarity of hillslopes systematically increases as gradients approach 1.2. These results are hard for me to reconcile with those of Grieve et al. In

25 particular, I am concerned that none of the R^* values in Figure 3a of Grieve et al. appear to
be larger than 0.7. This seems to suggest that Grieve et al. did not consider hillslopes steeper
than approximately $0.7 * 1.2 = 0.84$. However, we know that hillslopes steeper than 0.84 are
common in OCR. Grieve et al. argue that their results differ from those of Roering et al. due to
the different methods for extracting L_H . However, I don't think this adequately addresses the
30 fact that Roering et al.'s slope data clearly show the presence of gradients approaching 1.2 and
an increasing planarity of hillslopes as the gradients approach 1.2 in OCR, strongly indicating
that S_c is approximately 1.2 in that area. Grieve et al. would likely argue that S_c takes on a
range of values, hence the presence of some slopes with gradients above 1.0 or 1.1 does not
contradict their conclusion that the average S_c value is 0.79. Maybe this is true, but I would
35 like to see this hypothesis explored in more detail because I find the results of Roering et al.
(1999) very convincing in regard to the S_c value they chose.

As detailed in Grieve et al. (2016), the critical gradient which we constrain using these techniques
is necessarily an averaged value, as the fitting procedure will pass the steady state curve through
40 the center of the cluster of data points. This results in a critical gradient where approximately 50%
of the hillslopes will exceed the best fit S_c . Other attempts to constrain S_c have been made using
similar best fit methods (DiBiase et al., 2010; Hurst et al., 2012, 2013) which have found similar
underestimates in landscapes when contrasted with the value used by Roering et al. (1999). As noted
by the reviewer we argue that our best fit S_c value is the average value of a probability distribution
45 of critical gradients, whereas the value of Roering et al. (1999) can better be considered as an upper
bound S_c and should that value be required in a study, the methods of Roering et al. (1999) would be
better employed. Our method has the advantage of requiring little user supervision and no field data
to constrain an average S_c value and as such can facilitate rapid, broad scale comparisons between
landscapes.

50 We have rewritten the discussion of these points in the manuscript in order to better convey our
distinction between different definitions of S_c , in particular we have explicitly made the distinction
between the techniques for extracting S_c and have outlined why we observe differences between
the results of the methods. The explicit comparison between the S_c values of the 2 methods for the
Oregon Coast Range and Gabilan Mesa has also been removed from the discussion, to allow the
55 intercomparison of different best fit methods, rather than the comparison between an average and a
maximum value being made. We have also added a sentence at the end of the discussion to urge the
reader to consider which value of S_c is suitable for a given study.

In particular, I am concerned that none of the R^* values in Figure 3a of Grieve et al. appear
60 to be larger than 0.7. This seems to suggest that Grieve et al. did not consider hillslopes steeper
than approximately $0.7 * 1.2 = 0.84$. However, we know that hillslopes steeper than 0.84 are

common in OCR. Grieve et al. argue that their results differ from those of Roering et al. due to the different methods for extracting L_H .

In the original Roering et al. (2007) work, the upper limit of R^* calculated for the Oregon Coast Range was approximately 0.8, which yields a maximum gradient of 0.96, or a difference between these two gradients of 0.12. Aside from the previously highlighted difference in methods for measuring L_H and R between the two works, which result in a small increase in R and a larger increase in L_H (which has a net result of decreasing R^*), two other factors will influence the observed R^* values. Firstly, the spatial averaging will act to dampen the extreme values (both high and low), which can be seen by looking at the changes in the range of data points between Figure 5B and 5C and secondly, as demonstrated by Hurst 2012, any hilltops with a gradient above 0.4 must be excluded in order to use hilltop curvature as a proxy for erosion rate.

(2) Why might the Grieve et al. approach be flawed enough to provide a misleading measure of Sc and/or an incorrect assessment of steady state? I can think of at least four possibilities. First, the Oregon Coast Range may not be sufficiently in local topographic steady state for their method to apply at the necessary level of precision required for the presence/absence of topographic steady state and the value of Sc to be reliably determined (see, e.g., Sweeney et al., How steady are steady-state landscapes? Using visible–near-infrared soil spectroscopy to quantify erosional variability, Geology, 2012). In particular, their assumption that landscape-scale erosion rates can be extracted from the hilltop curvature seems to assume a topographic steady state and/or a uniformity of erosion rates that may not apply anywhere at the scale they are working.

In this paper we employ the same definition of steady state as was used in Grieve et al. (2016), whereby we consider a hillslope which retains a constant topographic form in relation to its baselevel, the channel at the base of the hillslope, to be in steady state. Such a formulation, defined by Mudd and Furbish (2004), and employed on a range of transient landscapes by Hurst et al. (2012, 2013) within the context of E^*R^* analysis, allows for the extraction of erosion rates across diverse tectonic and erosional regimes using hilltop curvature.

The clustering of the values in E^*R^* space when contrasted to transient landscapes such as Cascade Ridge (Figure 4) give us confidence that the Oregon Coast Range is in approximate steady state. We consider the variability which we observe in the E^*R^* data in such a landscape to highlight the catchment scale variability which has been predicted in models (Reinhardt and Ellis, 2015) and elegantly demonstrated with field data by Sweeney et al. (2012).

We have updated the theory section to include this explicit definition of steady state with the aim of increasing the clarity of our later discussions surrounding landscapes which are in steady state,

such as the Oregon Coast Range.

Second, they are applying a 1D model (equation (5)) to 2D reality. This may seem like a quibble, but the fact that there is nothing like a convergent hillslope in their model seems relevant in assessing its ability to definitively allow us to make conclusions regarding relatively subtle aspects of landscape evolution.

The challenge of applying 1D models to 2D reality is one which we should have explicitly addressed in this manuscript. The data generation and topographic analysis is designed to ensure that we are best able to apply these 1D models to our 2D data by following the methodology of Hurst et al. (2012), who first encountered this challenge. The valley extraction algorithm we employ, which is designed after Pelletier (2013) and Passalacqua et al. (2010) identifies areas of high convergence on hillslopes as valleys, which, when used as the end points for the flow routing algorithm employed to generate L_H and R measurements effectively exclude hillslope traces which cross convergent topography. We have added to the theory section of the paper to address this factor explicitly, presenting a brief review of methods of applying 1D models to 2D topography, and directing the reader to consider our results within the context of the challenges inherent in analyzing real topographic data.

Third, they assume that colluvial transport flux is independent of soil thickness. If sediment flux is an increasing function of soil thickness (as has been shown by many studies) and soil thickness is lower than the landscape average near divides (also common, since divides are divergent yet hillslopes includes convergent areas where soils tend to be thicker), then the approach of Grieve et al. may systematically overestimate the true value of E^* since the value of K will be an underestimate for the landscape as a whole. More broadly, equation (5) is of uncertain applicability if sediment flux is a function of soil thickness, bringing to my mind the question of how confident we can be in the results of this method with regard to the presence/absence of steady state.

The reviewer correctly highlights that there is evidence for depth dependent sediment transport on many hillslopes (e.g., Braun et al., 2001). Roering (2008) performed a non-dimensionalization of sediment transport from depth dependent creep and demonstrated an increased sensitivity of hilltop curvature to erosion rates under this transport regime. Which could be used to account for an increase in E^* values in a landscape. Unfortunately it is not currently possible to perform large scale experiments using real topography incorporating a depth-slope product flux law as we do not have soil thickness information at the spatial scale required.

Grieve et al. (2016) used topography to falsify predictions of the linear and nonlinear sediment flux models, but was unable to make any predictions regarding other sediment flux models due to either a lack of analytical solutions to the models, or as is the case for the depth-slope product, a lack of soil thickness information. The resulting work demonstrated that topography in four fieldsites was consistent with a nonlinear sediment flux law and this is the basis with which we employ such a model in this study, which shares the same fieldsites.

In light of this clear limitation to our results we have extended the Theoretical Background section to discuss the existence of other flux laws, and the basis of our selection of the nonlinear model over any of the other choices. We do not consider it possible to quantify the uncertainty in our results as we have no constraint on soil thickness, but trust that by drawing readers to this limitation near the start of the manuscript we can avoid any misunderstanding of the applicability of both our results and the technique as a whole.

A fourth possibility is that some fluvial erosion occurs on hillslopes in addition to colluvial erosion. As a result, their model (which includes erosion by colluvial processes only) might underestimates the true erosion rate. I think all of these possibilities should be considered in the analysis or at least acknowledged as possibilities in the revision.

This is a fundamental observation which impacts upon many facets of topographic analysis. In the case of this study we have taken great care to employ a valley extraction scheme based on the work of Pelletier (2013) and Passalacqua et al. (2010) which performs well across a range of landscapes in defining the transition point between channel and hillslope. However, no such algorithm is perfect when applied to real topographic data and as such we have expanded our methods section to more explicitly address this particular limitation of our topographic analysis.

Minor: The paper has a few typos. For example, “couple” should be “coupled” on p. 14, line 19. The publication year of Grieve et al. (2015) should be (2016). All of the references have strange random numbers included after them. These should be removed.

We have corrected these typos and a small number of other mistakes which were noticed during the typesetting process. The strange random numbers included after the references appear to have been added during the typesetting process, but we are investigating how to ensure that they do not appear in the final manuscript.

I wish to thank the authors for a stimulating paper and wish them the best as they continue on.

Review 2

Grieve and others present a method and software for linking erosion and the relief structure of landscapes. The manuscript is clearly written and the sensitivity analyses provide a useful guide to aid in interpreting the results of their method. Hence, I think this manuscript will be a useful and well-received contribution; the authors have produced a software that will benefit the community. Thank you.

We would like to thank the reviewer for their detailed consideration of our manuscript. We are pleased that the reviewer sees merit in the software we have produced, and agree that our sensitivity analyses should help the community to better interpret $E^* R^*$ measurements. Following the recommendations of this review we have modified Figure 5 to correct an error in how we labeled the subplots and have added a new figure to aid with the interpretation of the Coweeta results. We have expanded our discussion in several places to allow for possible alternative explanations of our results and have also implemented all of the minor edits suggested. We believe that these changes have significantly improved the quality and clarity of our manuscript. We respond to each point made by the reviewer individually below.

One comment regards the interpretation of data that do not fall on the Roering et al. (2007) curve. In the case of the Oregon Coast Range this could be either because 1) the landscape is in a steady state and the parameterization requires adjustment or 2) the landscape is not in a steady-state and the parameterization is correct. I suspect it is quite difficult to clearly distinguish among these two possibilities, and that both should be discussed in the manuscript.

The reviewer is correct that it is challenging to distinguish between these possibilities purely from topographic data. However, there is a considerable amount of evidence for the Oregon Coast Range being in steady state (e.g., Reneau and Dietrich, 1991; Roering et al., 2007) and the selection of a lower average S_c value is supported by earlier work to constrain the critical gradient (Grieve et al., 2016). We have added a sentence to the discussion of the Oregon Coast Range results to highlight this possible alternative interpretation: *‘This can be interpreted as evidence for topographic decay, however due to the preponderance of evidence supporting a steady state hypothesis for this landscape (e.g., Reneau and Dietrich, 1991; Roering et al., 2007), it is also possible that a critical gradient of 1.2 is too large in this location.’*

In responding to reviewer 1 we have also addressed these points more broadly, by expanding on our theory section and explicitly stating our definition of steady state. The challenges of parameterizing the model and fitting the critical gradient are now discussed in more detail in the manuscript,

with the aim of drawing the reader's attention to the potential limitations inherent within this method.

210 **Similarly, for the Coweeta site, there should be some justification for a substitution of the S_c**
value from the Oregon Coast Range for the value calculated from the framework,

Our selection of this value is based on the similarities in landscape morphology, sediment transport processes and the range of E^* values observed at the two sites. The aim of this selection of a
215 critical gradient is not to suggest that this is the correct value for Coweeta, but rather that a larger critical slope than the value 0.57 of reported in Grieve et al. (2016) produces data consistent with topographic decay. We have rewritten this section to better reflect that we do not claim that 0.79 is the correct value, rather that it is within a more plausible range than the value of 0.57.

220 **and more explanation of how the field observations indicate alluviation is reducing the critical gradient in this landscape.**

When we referred to the mean gradient reducing we should have instead referred to the mean relief reducing, which has the consequence of reducing the gradient. In locations where valley alluviation
225 is occurring, the base of the hillslope is raised vertically with regard to the elevation of the ridgeline. This reduces the relief whilst not changing the morphology of the hillslope, due to the difference in timescales of hillslope and channel response (Hurst et al., 2012). This can result in a reduction in R^* values across a landscape, leading to a lower S_c value being generated for a landscape than would be predicted were the alluviation not taking place. We have clarified this position and added
230 a more detailed explanation of this mechanism: *'As a valley fills with sediment, the hillslope relief will be reduced more rapidly than other hillslope properties, due to the difference between rates of hillslope and channel response to forcing (Hurst et al., 2012). Such a reduction in relief will reduce R^* , resulting in a reduced best fit S_c value.'*

235 **An additional comment is that results from this framework shown in Table 1 suggests there is little variation in S_c among the landscapes that were examined, despite differences in the setting of each site. I think this is a discussion point that could be elaborated upon.**

We have added to the discussion to raise this point, highlighting that it is a function of the ranges
240 of E^* and R^* values we observe in these landscapes, and that similar studies have arrived at the same magnitude of values for critical gradient. The following paragraph has been added to the critical gradient section: *'The similarity of the average S_c values obtained using the bootstrapping procedure across three diverse landscapes highlights the presence of a distribution of $E^* R^*$ values existing for each landscape, and the nature of an average S_c measurement. Such a distribution occurs due*

245 *to local variations in topography, process and material properties and similarities can be drawn
between the results presented in Table 1 and other similar studies (DiBiase et al., 2010; Hurst et al.,
2012).'*

**The comments and requests from the first reviewer are well-posed and reasonable, and
250 should also be weighed by the authors.**

We have made significant alterations to the manuscript following the recommendations of re-
viewer 1, details of which can be found in our response to that review.

255 **Minor comments: I encourage the authors to search the manuscript for “data is” and re-
place these instances with “data are”.**

We have made the requested changes.

260 **Page 3. Line 10. “methods published” – this sentence could be rephrased, it is slightly awk-
ward**

We have rephrased this sentence to better convey our meaning: *‘Such fundamental relationships
provide important insight into landscape evolution, however many of these techniques are challeng-
265 ing to implement, due to variable or poorly defined methods, or require proprietary software to
obtain data.’*

**Page 5. Line 15. Be explicit here about what limits relief. It isn’t a critical angle per se, but
material strength.**

270

We have rephrased this section to highlight that the critical angle is controlled by material strength.

Page 7. Line 12. I suggest inserting a comma following “(2012)”

275 Done.

**Page 18. Lines 17-19. It would be useful to show these data in a figure, so that readers can
compare results from the two Sc values.**

280 We have produced an additional figure (Figure 6 in the new manuscript) which displays this data
and have incorporated the figure into our discussion of potential topographic decay in this location.

**Page 16. Line 21. Replace “This is” with “The high R^* values” or similar phrasing to be
more explicit.**

285

Done.

**Figure 5. The ordering and lettering of the panels does not parallel the order in the caption.
Check that the main text follows the revised ordering, when referring to this figure.**

290

The main text in the manuscript is consistent with the figure caption, and this was the intended ordering of the subplots. Consequently we have re-generated Figure 5 with the subplots in the correct order to reflect the text and the caption.

295 References

- Braun, J., Heimsath, A. M., and Chappell, J.: Sediment transport mechanisms on soil-mantled hillslopes, *Geology*, 29, 683–686, doi:10.1130/0091-7613(2001)029<0683:STMOSM>2.0.CO;2, <http://geology.gsapubs.org/content/29/8/683>, 2001.
- DiBiase, R. A., Whipple, K. X., Heimsath, A. M., and Ouimet, W. B.: Landscape form and millennial
300 erosion rates in the San Gabriel Mountains, CA, *Earth and Planetary Science Letters*, 289, 134–144, doi:10.1016/j.epsl.2009.10.036, <http://www.sciencedirect.com/science/article/pii/S0012821X09006451>, 2010.
- Grieve, S. W., Mudd, S. M., and Hurst, M. D.: How long is a hillslope?, *Earth Surface Processes and Landforms*, doi:10.1002/esp.3884, <http://onlinelibrary.wiley.com/doi/10.1002/esp.3884/abstract>, 2016.
- 305 Hurst, M. D., Mudd, S. M., Walcott, R., Attal, M., and Yoo, K.: Using hilltop curvature to derive the spatial distribution of erosion rates, *Journal of Geophysical Research: Earth Surface*, 117, F02017, doi:10.1029/2011JF002057, <http://onlinelibrary.wiley.com/doi/10.1029/2011JF002057/abstract>, 2012.
- Hurst, M. D., Mudd, S. M., Attal, M., and Hilley, G.: Hillslopes Record the Growth and Decay of Landscapes, *Science*, 341, 868–871, doi:10.1126/science.1241791, <http://www.sciencemag.org/content/341/6148/868>,
310 2013.
- Mudd, S. M. and Furbish, D. J.: Influence of chemical denudation on hillslope morphology, *Journal of Geophysical Research: Earth Surface*, 109, F02001, doi:10.1029/2003JF000087, <http://onlinelibrary.wiley.com/doi/10.1029/2003JF000087/abstract>, 2004.
- Passalacqua, P., Do Trung, T., Foufoula-Georgiou, E., Sapiro, G., and Dietrich, W. E.: A geometric framework
315 for channel network extraction from lidar: Nonlinear diffusion and geodesic paths, *Journal of Geophysical Research: Earth Surface*, 115, F01002, doi:10.1029/2009JF001254, <http://onlinelibrary.wiley.com/doi/10.1029/2009JF001254/abstract>, 2010.
- Pelletier, J. D.: A robust, two-parameter method for the extraction of drainage networks from high-resolution digital elevation models (DEMs): Evaluation using synthetic and real-world DEMs, *Water
320 Resources Research*, 49, 75–89, doi:10.1029/2012WR012452, <http://onlinelibrary.wiley.com/doi/10.1029/2012WR012452/abstract>, 2013.
- Reinhardt, L. and Ellis, M. A.: The emergence of topographic steady state in a perpetually dynamic self-organized critical landscape, *Water Resources Research*, 51, 4986–5003, doi:10.1002/2014WR016223, <http://onlinelibrary.wiley.com/doi/10.1002/2014WR016223/abstract>, 2015.
- 325 Reneau, S. L. and Dietrich, W. E.: Erosion rates in the southern oregon coast range: Evidence for an equilibrium between hillslope erosion and sediment yield, *Earth Surface Processes and Landforms*, 16, 307–322, doi:10.1002/esp.3290160405, <http://onlinelibrary.wiley.com/doi/10.1002/esp.3290160405/abstract>, 1991.
- Roering, J. J.: How well can hillslope evolution models “explain” topography? Simulating soil transport and production with high-resolution topographic data, *Geological Society of America Bulletin*, 120, 1248–1262, doi:10.1130/B26283.1, <http://gsabulletin.gsapubs.org/content/120/9-10/1248>, 2008.
330
- Roering, J. J., Kirchner, J. W., and Dietrich, W. E.: Evidence for nonlinear, diffusive sediment transport on hillslopes and implications for landscape morphology, *Water Resources Research*, 35, 853–870, doi:10.1029/1998WR900090, <http://onlinelibrary.wiley.com/doi/10.1029/1998WR900090/abstract>, 1999.

- Roering, J. J., Perron, J. T., and Kirchner, J. W.: Functional relationships between denudation and hillslope
335 form and relief, *Earth and Planetary Science Letters*, 264, 245–258, doi:10.1016/j.epsl.2007.09.035, <http://www.sciencedirect.com/science/article/pii/S0012821X07006061>, 2007.
- Sweeney, K. E., Roering, J. J., Almond, P., and Reckling, T.: How steady are steady-state landscapes?
Using visible–near-infrared soil spectroscopy to quantify erosional variability, *Geology*, 40, 807–810,
doi:10.1130/G33167.1, <http://geology.gsapubs.org/content/40/9/807>, 2012.

A nondimensional framework for exploring the relief structure of landscapes

Stuart W. D. Grieve¹, Simon M. Mudd¹, Martin D. Hurst², and David T. Milodowski¹

¹School of GeoSciences, University of Edinburgh, Drummond Street, Edinburgh EH8 9XP, UK

²British Geological Survey, Keyworth, Nottingham NG12 5GG, UK

Correspondence to: Stuart W. D. Grieve (s.grieve@ed.ac.uk)

Abstract. Considering the relationship between erosion rate and the relief structure of a landscape within a non-dimensional framework facilitates the comparison of landscapes undergoing forcing at a range of scales, and allows broad scale patterns of landscape evolution to be observed. We present software which automates the extraction and processing of relevant topographic parameters to rapidly generate non-dimensional erosion rate and relief data for any landscape where high resolution topographic data ~~is~~are available. Individual hillslopes are identified using a connected components technique which allows spatial averaging to be performed over geomorphologically meaningful spatial units, without the need for manual identification of hillslopes.

The software is evaluated on four landscapes across the continental United States, three of which have been studied previously using this technique. We show that it is possible to identify whether landscapes are in topographic steady state. In locations such as Cascade Ridge, CA a clear signal of an erosional gradient can be observed. In the Southern Appalachians, non-dimensional erosion rate and relief data ~~is~~are interpreted as evidence for a landscape decaying following uplift during the Miocene. An analysis of the sensitivity of this method to free parameters used in the data smoothing routines is presented which allows users to make an informed choice of parameters when interrogating new topographic data using this method. A method to constrain the critical ~~graident~~gradient of the nonlinear sediment flux law is also presented which provides an independent constraint on this parameter for three of the four study landscapes.

1 Introduction

The Earth's surface evolves dynamically in response to the interplay of climatic, tectonic and other factors operating at timescales ranging from minutes to millenia. High resolution topographic data generated from terrestrial and airborne laser scanning, in combination with increased computational power has facilitated a revolution in geomorphology, allowing the quantitative interrogation of landscape form to provide insight into the forces shaping a landscape. Relationships have been found between topography and the tectonic (e.g., Wobus et al., 2006; Hilley and Arrowsmith, 2008; DiBiase

et al., 2012; Hurst et al., 2013a), climatic (e.g., Gabet et al., 2004; Anders et al., 2008; Champagnac et al., 2012) and biotic (e.g., Roering et al., 2010; Milodowski et al., 2015a) forcing of a landscape in addition to links between topography and bedrock properties (e.g., Korup, 2008; Clarke and Burbank, 2010, 2011; Hurst et al., 2013b).

Such fundamental relationships provide important insight into landscape evolution, however many of these techniques are challenging to implement, ~~require proprietary software or have varied due to variable~~ or poorly defined methods ~~published to obtain similar results, or require proprietary software to obtain data~~. This highlights the need for standardized techniques and tools to allow the analysis of topographic data to be reproduced and falsified, strengthening our understanding of the processes that shape planetary surfaces. In this contribution we focus on methods exploiting high resolution topographic data in soil mantled landscapes that aim to elucidate both sediment flux laws (c.f., Dietrich et al., 2003) and the transient evolution of landscapes (e.g., Hurst et al., 2013a).

Our approach is rooted in a non-dimensional framework that describes relationships between erosion rates and hillslope topography in soil mantled landscapes (Roering et al., 2007). This framework facilitates the direct comparison of landscapes of widely varying morphology and process. It has been shown to provide compelling insight into the identification of landscape transience (Hurst et al., 2012), complex tectonic signals from topography (Hurst et al., 2013a), and process controls on the density of channels (Sweeney et al., 2015). Extracting the nondimensional parameters from high resolution topography can be difficult, subject to choices about how the metrics are calculated, and there has been no investigation into how different methods might influence results, and therefore the interpretation of landscapes.

Here we present a framework and methodology for extracting the required topographic parameters and processing the resulting data. Our software uses a clear methodology to allow researchers to generate this data for new landscapes and can replicate published relationships between non-dimensional erosion rate and relief. Such relationships can be used to discriminate between landscapes in topographic steady state, where erosion rate is balanced by uplift rate, and those undergoing transience or topographic decay.

Additionally we present a method for generating spatially contiguous hilltop patches, required as a spatial averaging tool in many studies (e.g., Perron et al., 2009; Hurst et al., 2012, 2013a) to identify individual hillslopes for analysis. An analysis on the influence of spatial averaging and data smoothing on the interpretation of topographic data is undertaken and hillslope and basin average data ~~is-are~~ also used to estimate the critical gradient, a key parameter in the nonlinear sediment flux model.

2 Theoretical Background

~~One end-member sediment flux law is the nonlinear sediment flux law (Andrews and Bucknam, 1987; Roering et al., 1999, 2001, 2002).~~

Numerous sediment flux laws (cf. Dietrich et al., 2003) have been developed and tested, particularly since the advent of cosmogenic radionuclide dating and high resolution topographic measurements. In addition to the conceptually simple linear flux law (Culling, 1960; McKean et al., 1993; Tucker and Slingerland, 1997; Small et al. models of depth dependent (Braun et al., 2001; Furbish and Fagherazzi, 2001; Heimsath et al., 2005; Roering, 2008) and nonlinear sediment flux (Andrews and Bucknam, 1987; Roering et al., 1999, 2001, 2007) have been employed, alongside models which directly consider sediment particle motion (Foufoula-Georgiou et al., 2010; Tucker and Bradley,

Models which consider particle motion are challenging to apply to real topography as they do not have an analytical solution and without high resolution soil depth information it is challenging to apply a soil thickness based sediment flux law to landscape scale analysis (Grieve et al., 2016). However, topographic predictions of the nonlinear flux law have been successfully tested (Roering et al., 2007; Grieve et al., 2016) such that it, at a minimum, can constrain broad scale sediment transport processes across landscapes. The nonlinear flux law is (Andrews and Bucknam, 1987; Roering et al., 1999, 2001, 2007),

$$\bar{q}_s = \frac{KS}{1 - (|S|/S_c)^2}, \quad (1)$$

where S is the topographic gradient in dimensions of Length/Length (dimensions denoted in square brackets as $[L]$ length, $[M]$ ass and $[T]$ ime), S_c [dimensionless] is the hillslope critical gradient, K [L^2T^{-1}] is a sediment transport coefficient and \bar{q}_s [L^2T^{-1}] is a volumetric sediment flux per unit contour length. As S tends towards S_c , the sediment flux asymptotically increases towards infinity, corresponding to an increase in landsliding on an increasingly planar hillslope.

Roering et al. (2007) modeled the relief structure of theoretical one-dimensional hillslopes which evolve under Equation 1 and found that relief, the difference in elevation between a hilltop and the point on the channel it is coupled to, is controlled by the erosion rate, hillslope length and the sediment transport coefficient. Equation 1 has been found to be consistent with observations of topography and erosion rates across several landscapes (e.g., Roering et al., 1999, 2007; Roering, 2008; Hurst et al., 2012)

Roering et al. (2007) normalized relationships describing these one-dimensional hillslopes using topographic parameters to produce a dimensionless erosion rate,

$$E^* = \frac{E}{E_R} = \frac{\rho_r}{\rho_s} \cdot \frac{2EL_H}{KS_c} = \frac{-2C_{HT}L_H}{S_c} \quad (2)$$

where E [LT^{-1}] is the erosion rate, ρ_r and ρ_s [ML^{-3}] are the rock and soil bulk densities, respec-

tively, $C_{HT} [L^{-1}]$ is the hilltop curvature, $L_H [L]$ is the hillslope length, $E_R [LT^{-1}]$ is a reference erosion rate denoted as:

$$E_R = \frac{K S_c}{2L_H(\rho_r/\rho_s)}, \quad (3)$$

95

and the dimensionless relief is given as:

$$R^* = \frac{R}{S_c L_H}, \quad (4)$$

where $R [L]$ is the topographic relief. Parabolic hillslope profiles are generated when E^* values are less than or equal to one, such that R^* increases approximately linearly with erosion rate. Planar hillslopes near the critical gradient, S_c , indicate that R^* is insensitive to erosion rate when E^* approaches or exceeds one. This prediction is consistent with observations that when erosion rates are high, relief becomes limited by a critical slope angle, [set by the material properties of the underlying bedrock](#) (e.g., Binnie et al., 2007; DiBiase et al., 2012). A combination of high E^* and R^* values indicates a landscape with steep, planar hillslopes and frequent landsliding whereas low values suggest more convex hillslopes with lower overall relief (Roering et al., 2007).

For landscapes in topographic steady state with uniform erosion rates, values of E^* and R^* will plot on the steady state curve described by:

$$R^* = \frac{1}{E^*} \left(\sqrt{1 + (E^*)^2} - \ln \left(\frac{1}{2} \left(1 + \sqrt{1 + (E^*)^2} \right) \right) - 1 \right). \quad (5)$$

110

[Here, we define steady state using the formulation of Mudd and Furbish \(2004\) which considers a hillslope to be in steady state if it retains a constant topographic form with regard to its local baselevel, the channel at its base.](#) Steady state hillslopes which experience spatially uniform erosion rates will plot on a single point on the curve (Roering et al., 2007), whereas landscapes experiencing

115

an erosion gradient will plot at many points along this curve, as demonstrated by Hurst et al. (2012). These non-dimensional landscape properties have utility beyond steady state landscapes. Hurst et al. (2013a) used this formulation to distinguish between growing and decaying parts of a landscape by identifying hysteresis in $E^* R^*$ space. Sweeney et al. (2015) has applied similar techniques to analogue landscape evolution models to demonstrate that the efficiency of hillslope sediment transport controls drainage density. These cases of differing landscape properties and histories highlight the power of using topography and $E^* R^*$ analysis to interpret landscape evolution.

120

[The application of such a framework to real data is limited by the challenge of applying a one-dimensional model of hillslope evolution to two-dimensional topographic data. Attempts to apply such models](#)

typically identify non-convergent portions of the landscape upon which to perform tests either through field surveying planar hillslopes (Rosenbloom and Anderson, 1994), the algorithmic identification of convergent topography (Grieve et al., 2016), manual identification of planar topography from digital elevation models or the exclusion of areas of high convergence from hillslope profiles through a valley extraction algorithm as is employed by Hurst et al. (2012) and in this study. All such methods are compromises between computational efficiency, reproducibility and the accuracy with which a one-dimensional hillslope profile can be extracted. Consequently the conclusions drawn using this, or any other, application of one-dimensional to two-dimensional data must be considered within the context of their potential errors.

3 Hilltop patches

The extraction of signals from high resolution topographic data can often require smoothing of raw data to filter out both topographic and artificial noise (Lashermes et al., 2007; Roering et al., 2010; Sofia et al., 2013). This smoothing can be performed either by processing the raw DEM before any analysis is performed (e.g., Roering et al., 2010), or by smoothing the output data (e.g., Tucker et al., 2001; Tarolli and Dalla Fontana, 2009). In order to understand landscape properties at a hillslope scale it is often desirable to perform local smoothing to group individual DEM pixels into collections of pixels that correspond to individual hilltops and their connected hillslopes.

This was performed by Hurst et al. (2012) through a process of vectorizing hilltops, then splitting the vectors by a threshold length and discarding all split segments shorter than an arbitrary length of 50 meters. The final split vectors are then converted back into rasters, to create a network of hilltop patches of a defined minimum length. These patches are typically 2 pixels wide, spanning both sides of a drainage divide. This technique is challenging to reproduce, as it relies upon several user defined parameters and a subjective assessment of which vector segments to discard.

3.1 Automated generation of hilltop patches

Connected components analysis is a technique typically used in computer vision to label contiguous pixels in raster images (e.g. Rosenfeld and Pfaltz, 1966; Samet, 1981; Lumia et al., 1983; Dillencourt et al., 1992; Suzuki et al., 2003; He et al., 2013). Here, we implement a computationally efficient connected components algorithm developed by He et al. (2008) to generate contiguous hilltop patches, resulting in a network of hilltop patches, each coded with a unique ID number. Finally, in order to allow better replication of the original concepts used in Hurst et al. (2012), a minimum patch area can be supplied, which is used to remove any hilltop patches which are smaller than this user defined threshold.

This hilltop patch identification method is very efficient and has been demonstrated to operate effectively on large, complex images (He et al., 2008) without an impact on performance. This

technique has utility beyond E^*R^* calculations, as it can be used in any work where discrete patches of hilltop need to be identified (e.g., Perron et al., 2009) or where individual hillslopes must be analyzed using topographic data.

4 Generating topographic data

4.1 Extraction of a channel network

A key component of most topographic analysis is the delineation of a channel network, without which many topographic parameters cannot be estimated. Channel networks can be extracted either by using a process based method which uses the stream power model to identify the point in a landscape where fluvial processes begin to dominate over hillslope processes (Clubb et al., 2014) or by using a geomorphometric method which identifies channels using curvature thresholds (Passalacqua et al., 2010; Orlandini et al., 2011; Pelletier, 2013).

In order for the E^*R^* data to capture the true range of erosion rates and reliefs inherent in a landscape, it is important to define a channel network which correctly identifies the hillslope-fluvial transition, including the delineation of colluvial channels which are often challenging to identify using non-geomorphometric methods (Pelletier, 2013). Here we follow Pelletier (2013) and apply a Wiener filter (Wiener, 1949) to remove noise from the raw topographic data. Subsequently, channelized portions of the drainage network are identified based on a tangential curvature threshold (e.g., Pelletier, 2013). The appropriate curvature threshold is identified from the properties of its quantile-quantile plot (e.g., Lashermes et al., 2007; Passalacqua et al., 2010). These channelized patches of the landscape are combined by performing a connected components analysis (He et al., 2008) which merges discrete patches of channel into a contiguous channel network. Following methods outlined in Grieve et al. (2016) floodplain masks are also created and combined with this channel network, which separates the landscape into two domains; hillslopes and channels. This has the effect of terminating hillslope traces when they reach a hollow or enter the floodplain, ensuring that the trace properties only reflect the hillslope domain and the E^*R^* measurements are not contaminated by sampling parts of the landscape which the nondimensional framework does not apply to.

If the channel network is incorrectly defined, some fluvial erosion could impact the correct measurement of E^*R^* values. However, due to the number of individual measurements per landscape (> 160000 in each case) and the small number of points on a landscape where such erroneous measurements could occur, such measurements will have little impact on landscape scale trends, particularly when spatial averaging is applied.

4.2 Extraction of topographic parameters

All of the key measurements required to generate E^*R^* data can be extracted from high resolution topography (Roering et al., 2007). Calculation of E^* using Equation 2 requires hillslope length and

hilltop curvature, and calculation of R^* using Equation 4 requires the relief and hillslope length to be measured from high resolution topography.

[Grieve et al. \(2016\)](#) measured hillslope length by generating overland flow paths running from hilltop to channel pixels for every hilltop in a DEM, thereby generating a diverse range of measurements shown to characterize the range of hillslope properties inherent within a landscape. From these traces, each hilltop's local relief is also measured by taking the difference between the elevation at the start (hilltop) and end (channel) of each trace. Finally, the hilltop curvature for each hilltop pixel is extracted following Hurst et al. (2012) whose techniques demonstrated that hilltop curvature scales linearly with erosion rate below hilltop gradients of 0.4. Correspondingly, we also sample the hilltop gradient (S_{HT}) at the start of each trace, to allow data to later be filtered by this value. By using the methods outlined by [Grieve et al. \(2016\)](#) we can generate a four-tuple of information for each hilltop pixel in the landscape containing (L_H, R, C_{HT}, S_{HT}) .

4.3 Smoothing topographic parameters

In previous studies that generate $E^* R^*$ data, some form of smoothing has been employed to extract meaningful trends from the inherently noisy topographic data. Roering et al. (2007) hand selected basins with uniform morphologies and minimal anthropogenic disturbance to measure topographic parameters from, effectively removing the majority of noise in the landscape and producing a small number of data points considered to be characteristic of their 2 steady state landscapes.

Hurst et al. (2012) used semi-automated methods to extract the required topographic parameters, and averaged the resulting data spatially over hilltop segments of a defined minimum length. Hurst et al. (2013a) utilized the same methodology, but further averaged the data by grouping segments into bins defined by their distance along the Dragon's Back Pressure Ridge, to explore the topographic expression of a transient uplift signal along the ridge. As these techniques do not self select idealized hillslopes or basins as in Roering et al. (2007) some filtering of the raw data was required (see Section 5.1). These latter methods allow $E^* R^*$ data to be used to interrogate transient landscapes, increasing the power of the method and providing a vital tool in the topographic analysis of landscapes.

Here, we extract topographic parameters from raw topographic data and smooth the resulting measurements, in accordance with previous authors' methods, firstly performing spatial averaging at a basin scale. The basins that are used to average the topographic parameters can be defined in an automated manner to produce an average value over all basins of a given stream order, or a more user defined approach can be undertaken to select basins manually, in order to more closely replicate the work of Roering et al. (2007). Secondly the parameters can be averaged at a hillslope scale by using the discrete hilltop patches generated using the technique outlined in Section 3.1. The data ~~is~~ [are](#) filtered using the same constraints outlined in Hurst et al. (2012), removing hilltops with a $S_{HT} > 0.4$ or a patch size < 50 meters, with the additional filtering of hillslope length and relief values below a user defined threshold, typically 2-5 meters for each parameter; this ensures that hilltops

sampled are true hilltops and are not interfluvies sitting adjacent to a basin outlet, which will not conform to models of hillslope sediment transport. The data ~~is~~are also returned to the user filtered, but not averaged, allowing users to explore the raw data to ensure that the smoothed data ~~is~~are a good reflection of the overall trends inherent in a landscape.

5 Processing the topographic data

Once the topographic data has been extracted, it is filtered to ensure that only data which conforms to the nondimensional framework described by Roering et al. (2007) is used in any further analysis.

5.1 Filtering

The key filtering process which must be performed is the removal of any data points which have an S_{HT} above 0.4. This threshold gradient was shown by Hurst et al. (2012) to be the point at which hilltop curvature stops scaling linearly with erosion rate, for a range of K values representative of values published for our fieldsites (Roering et al., 1999, 2007; Matmon et al., 2003; Hurst et al., 2012), and therefore cannot be used in Equation 2 as a proxy for erosion rate. Across all of the datasets, gradients which exceed 0.4 are removed from further analysis. In the case of the two spatially averaged datasets individual hilltop pixels which exceed this threshold gradient within a patch or basin, are removed from the averaging process for each measurement ensuring that no invalid data contributes to the final calculations. To ensure the validity of each basin average measurement, a count of the valid pixels contained within each basin following gradient filtering is performed and any basins with fewer valid measurements than a user defined threshold can be removed from the analysis. This threshold is typically equal to the minimum patch size used in Section 3.1 as this provides consistency between measurements.

5.2 Log binning

One method of non-spatial averaging of geomorphic data used effectively to generate slope-area plots (e.g., Tarolli and Dalla Fontana, 2009) is log-binning. Such a method provides an opportunity to interrogate the data at a landscape scale while still removing the noise inherent in topographic measurements. Each E^*R^* pair is placed into evenly spaced bins in base 10 logarithmic space. The bin spacing is a function of the number of bins specified by the user and the range of E^* values within the dataset and its impact on interpretation of the data is considered in Section 6.2.3. To ensure that a valid number of data points make up each bin, a minimum bin size can also be specified by the user, this value will depend on the size and nature of the dataset.

This type of averaging will work best in landscapes where an erosion gradient is expected, as it will produce a range of E^*R^* values across the domain, as can be seen in Hurst et al. (2012). In presumed steady state locations such as Gabilan Mesa most of the data ~~is~~are expected to cluster

around a single point (Roering et al., 2007), and so imposing evenly spaced bins in log space onto such data may construct an artificial trend. It is therefore recommended to consider the raw data in conjunction with the binned data to ensure that the trends in the data are valid.

5.3 Visualizing data

265 The software allows the user to plot any combination of the E^*R^* datasets, facilitating the rapid generation of basin and landscape average data following Roering et al. (2007), hilltop averaged and log binned data following Hurst et al. (2012, 2013a) and raw data which has previously not been available. It is also possible to interrogate the raw measurements as a density plot, which more accurately conveys the trends in the raw data as in large landscapes many measurements share the
270 same location in E^*R^* space. By allowing simple inter-comparisons between plotting methods it becomes trivial to assess the most suitable data visualization techniques for a specific landscape.

6 Results and ~~Discussion~~discussion

By using data from previous studies which utilize E^*R^* analysis it is possible to assess the ability of this software to reproduce existing results in addition to understanding how the varying techniques
275 for smoothing the data, discussed in Section 4.3, can impact on the interpretation of the processes operating on a landscape. Four landscapes in the continental USA have been selected to evaluate the software, the Oregon Coast Range and Gabilan Mesa, used by Roering et al. (2007), Cascade Ridge, used by Hurst et al. (2012) and the Coweeta Hydrologic Laboratory (Figure 1). High resolution LiDAR data ~~is~~are available from the National Center for Airborne Laser Mapping (NCALM) for
280 each site and each site's point cloud data has been gridded to 1 meter resolution DEMs following Kim et al. (2006) and accuracy information for each point cloud can be found in Appendix A.

6.1 Reproducing previous work

6.1.1 Oregon Coast Range and Gabilan Mesa

The Oregon Coast Range in Oregon, USA is a steeply incised upland landscape with dense forest
285 cover and a humid climate (Roering et al., 1999), leading to frequent debris flows, which initiate in colluvial hollows (Stock and Dietrich, 2003). The forests of the Oregon Coast Range are dominated by hardwoods, such as Oregon Maple (*Acer macrophyllum*), and coniferous forest such as Douglas Fir (*Pseudotsuga menziesii*) (Schmidt et al., 2001). Extensive work has been carried out to estimate the uplift rate of the range using marine terrace data (Kelsey et al., 1996), and these estimates of
290 uplift rate correspond to erosion rates measured using cosmogenic radionuclides (e.g., Heimsath et al., 2001). This correspondence between uplift and erosion rate has been used to infer that the Oregon Coast Range is in steady state (e.g., Reneau and Dietrich, 1991; Roering et al., 2007).

Gabilan Mesa in California, USA is part of the Central Coast Ranges and has a semiarid Mediterranean climate with higher vegetation densities on northern slopes due to microclimatic variations (Dohrenwend, 1978). The vegetation of Gabilan Mesa is characterized by a combinations of oak savannah containing Blue Oak (*Quercus douglasii*) and chaparral shrubland containing Chamise (*Adenostoma fasciculatum*) (Shreve, 1927). The landscape is very smooth with a regular spacing of tributaries and valleys (Dohrenwend, 1978, 1979) and gentle transitions between hillslopes and channels, suggesting that diffusive processes dominate the transport of sediment on hillslopes (Roering et al., 2007). Hilltop curvature shows little variance across the landscape and in conjunction with the regularity of valley spacing, this suggests that the landscape is in approximate topographic steady state (Roering et al., 2007; Perron et al., 2009).

Roering et al. (2007) estimated the topographic parameters L_H , R and C_{HT} for the Oregon Coast Range and Gabilan Mesa fieldsites. The characteristic hillslope length for each landscape was estimated by identifying the inflection point in a spline curve fitted through a plot of local slope against drainage area. This inflection point is considered to correspond to the transition between the hillslope and channel domain in a landscape (Montgomery and Foufoula-Georgiou, 1993; Hancock and Evans, 2006; Tarolli and Dalla Fontana, 2009; Tarolli, 2014; Tseng et al., 2015).

Roering et al. (2007) estimated mean relief by calculating the mean of the differences between the maximum and minimum elevation within a kernel of radius equal to the characteristic hillslope length for each point on the landscape. Hilltop curvature was sampled from manually defined hilltops with a gradient below $0.05S_c$ and averaged across each landscape. The critical gradient was calculated for the Oregon Coast Range to be 1.2 by Roering et al. (1999) and Roering et al. (2007) assumed that this value is also correct for Gabilan Mesa.

The data from Gabilan Mesa (Figure 2A) reveals many hilltop patches which correspond closely to the predicted E^*R^* values from Roering et al. (2007). The data is predominantly clustered around a single point, showing strong agreement with observations that the landscape is in approximate steady state. However the majority of the basin average data points and a considerable amount of the hilltop patch data plots below the steady state curve, which could be interpreted as evidence for topographic decay. However the uniform hilltop curvatures and valley spacing, coupled with measurements of long term erosion rates suggest that this landscape is not undergoing topographic decay (Roering et al., 2007; Perron et al., 2009). An alternative explanation for the data falling below the steady state curve is that an S_c value of 1.2 is too large for this landscape. Grieve et al. (2016) used similar topographic parameters to estimate the critical gradient for this landscape as 0.8. By replotting this data using this revised S_c , the data plots more closely to the steady state curve (Figure 2B).

The Oregon Coast Range data is more tightly constrained than the Gabilan Mesa Data (Figure 3A), and has a similar range of R^* values. However, as is the case for Gabilan Mesa, the majority of the data plots below the steady state curve. This can be interpreted as evidence for topographic decay.

however due to the preponderance of evidence supporting a steady state hypothesis for this landscape (e.g., Reneau and Dietrich, 1991; Roering et al., 2007), it is also possible that a critical gradient of 1.2 is too large in this location. By using the S_c value of 0.79 constrained by Grieve et al. (2016), the data moves closer to the steady state curve (Figure 3B). Using this average S_c value several R^* measurements exceed 1. This indicates that these hillslopes are too steep to sustain soil mantle in this landscape, which corresponds to field observations of the Oregon Coast Range, where frequent shallow landsliding is reported (e.g., Benda and Dunne, 1997; Montgomery et al., 1998) and where periodic wildfires expose large (tens of m^2) patches of bedrock (Jackson and Roering, 2009).

As acknowledged by Roering et al. (2007) extracting the relief from a moving window fails to capture the complete range of relief values in a landscape, resulting in an average value which dampens the true signal, reducing R in high relief landscapes such as the Oregon Coast Range. Our method of measuring relief of individual hillslope traces circumvents this problem.

The majority of the data points in Figures 2 and 3 have larger E^* values than those from Roering et al. (2007). Grieve et al. (2016) showed that estimating L_H using slope-area plots systematically underestimates L_H by as much as an order of magnitude in some landscapes. Such an underestimate would reduce the E^* value for a landscape and explains the systematic differences between this study and the results of Roering et al. (2007). The larger range of hilltop patch data highlights the range of E^*R^* values inherent in even a uniform landscape which is in approximate topographic steady state.

6.1.2 Cascade Ridge

Cascade Ridge is a section of the Northern Sierra Nevada in California, USA. The landscape is predominantly forested and the climate is semi-arid (Hurst et al., 2012). The characteristic topographic form of this landscape is a smooth, low relief relict surface which is heavily incised, creating steep canyons with an irregular spacing. The plateau surface is vegetated with oak forest including California black oak (*Quercus kelloggii*) and canyon live oak (*Quercus chrysolepis*) and pine forest containing ponderosa pine (*Pinus ponderosa*), Douglas fir (*Pseudotsuga menziesii*) and sugar pine (*Pinus lambertiana*), whereas the canyon is dominated by chaparral vegetation such as manzanita (*Arctostaphylos spp*) (Gabet et al., 2015; Milodowski et al., 2015a). These contrasting landscape morphologies have been shown to be eroding at different rates, with the plateau surfaces eroding an order of magnitude more slowly than the canyons (Riebe et al., 2000; Hurst et al., 2012). This produces a complex landscape exhibiting a range of erosion rates influenced by climate and tectonic signals which is not in topographic steady state (Riebe et al., 2000; Stock et al., 2004; Hurst et al., 2012; Gabet et al., 2015).

Cascade ridge is a more morphologically complex landscape than the Oregon Coast Range or Gabilan Mesa, correspondingly, the E^*R^* data for this landscape is predicted to plot along the steady state curve at a broad range of E^* values, as was demonstrated by Hurst et al. (2012). Using

an S_c value of 0.8, as proposed by Hurst et al. (2012), produces data spanning a much wider portion of E^*R^* space than the data for the steady state landscapes of Gabilan Mesa and the Oregon Coast Range (Figure 4A). The binned hilltop patch data shows good agreement with the data from Hurst et al. (2012), spanning a similar range of E^* values with the steady state curve falling within the standard error of each bin. This supports observations of a range of erosion rates and landscape morphologies and highlights the utility of this method in gaining a first order approximation of the tectonic and erosional setting of a landscape where no field data ~~is~~are available.

At the Cascade Ridge site, ~~?~~Grieve et al. (2016) estimated S_c to be 0.72, calculated from topographic parameters. Using this value there is little change in the trends in the data (Figure 4B), most of the points now fall above the line and at high values of E^* , and more data points have R^* values in excess of 1. ~~This is~~ These high R^* values are consistent with field observations of this transient landscape wherein rapid valley downcutting may decouple hillslopes from the channel network (Milodowski et al., 2015b) and drive shallow landsliding. In a complex landscape such as Cascade Ridge, which is known to have a broad range of erosion rates and hillslope morphologies, a landscape average S_c value will regress towards the mean. Consequently, as more of the landscape is covered by the low gradient plateau than the steeper canyons, the S_c value of 0.72 does not reflect the parts of the landscape with larger E^*R^* values, which may fall closer to the value of 0.8 used by Hurst et al. (2012).

6.1.3 Coweeta

The Coweeta Hydrologic Laboratory is in the Southern Appalachian Mountains in North Carolina, USA and is a densely vegetated landscape which exhibits classic ridge and hollow topography (Hales et al., 2012). Such topography produces many source areas for shallow landslides in colluvial hollows, which are triggered by high intensity storms connected to hurricanes ~~(?)~~ (Swift Jr. et al., 1988). The vegetation at Coweeta is a mix of shrubs, such as *Rhododendron maxima*, and Northern Hardwood forest, the distribution of which is controlled by wildfires which in many cases are managed through human intervention (Hales et al., 2009). It is debated whether the Southern Appalachians are in topographic steady state, as there is little tectonic activity, yet there is a large amount of relief preserved across the range (Baldwin et al., 2003; Matmon et al., 2003; Gallen et al., 2011, 2013).

The Southern Appalachian Mountains have never previously been investigated using E^*R^* methods and so can be used to evaluate the technique's ability to interrogate a complex landscape and assist in the interpretation of topographic signals. Figure 5 outlines the range of methods which can be used to interpret E^*R^* data. As in Sections 6.1.1 and 6.1.2 the critical gradient used is taken from ~~?~~ Grieve et al. (2016). The raw data in Figure 5A shows the range of reliefs observed in the Southern Appalachians. The landscape median E^*R^* value falls within the zone of maximum probability density, this highlights the level of noise inherent in high resolution topographic data when

interrogating them in E^*R^* space, outlining the requirement to smooth or bin the data in order to extract meaningful information from the topographic data.

Comparing Figure 5B and 5C to data for steady state landscapes such as Gabilan Mesa or the Oregon Coast Range shows similar levels of clustering, with the location of the cluster of patch and basin average values corresponding with the Oregon Coast Range data (Figure 3). This corresponds well to field observations of hillslope morphology in these two locations, with planar hillslopes and frequent shallow landsliding reported (Benda and Dunne, 1997; Montgomery et al., 1998; Roering et al., 1999) and this clustering suggests that there is less spatial variation in erosion rate in Coweeta than in Cascade Ridge, an assertion supported by measured erosion rates from both locations (e.g., Riebe et al., 2000; Matmon et al., 2003; Hales et al., 2012; Hurst et al., 2012). Figure 5D shows the binned data for Coweeta and highlights the smaller range of E^* values for this landscape when compared to Cascade Ridge. It also draws attention to the need to analyze E^*R^* data using numerous methods to avoid an incorrect interpretation, as discussed in Section 5.2.

The Coweeta E^*R^* data clusters around a point on the steady state curve and it could be concluded that this landscape is in approximate steady state. However, the value of S_c used in Figure 5 is significantly smaller than any previously published S_c value. Field observations of Coweeta reveal that many channels are alluviated and such deposition at the base of hillslopes will ~~reduce the mean gradient~~ alter the mean properties of a hillslope, and move its idealized profile away from the model hillslopes defined by Roering et al. (2007). As a valley fills with sediment, the hillslope relief will be reduced more rapidly than other hillslope properties, due to the difference between rates of hillslope and channel response to forcing (Hurst et al., 2012). Such a reduction in relief will reduce R^* , resulting in a reduced best fit S_c value. Such an alteration of mean hillslope properties could explain the considerable underestimation of the critical gradient when it is constrained through hillslope length-relief relationships.

~~By selecting an S_c value of 0.79, taken from the~~ The Oregon Coast Range, ~~which is~~ a broadly similar landscape to Coweeta, based on the range of E^* values ~~and field observations~~, general landscape morphology and observations of sediment transport processes has a critical gradient of 0.79 (Grieve et al., 2016). This value is similar to the S_c of many other landscapes (DiBiase et al., 2010; Hurst et al., 2012; Grieve et al., 2013) as such we use this value to explore the patterns of E^*R^* in Coweeta when a larger critical gradient, which more closely resembles predicted values for other landscapes is employed. In such a case the majority of the data plots below the steady state curve (Figure 6). Hurst et al. (2013a) observed E^*R^* data plotting below the steady state curve along the Dragons Back Pressure Ridge, where these sections of the landscape are understood to be topographically decaying following a pulse of uplift. If this S_c is correct it could lend support to the idea of a Miocene rejuvenation of topography in the Southern Appalachians (Gallen et al., 2013) followed by a period of gradual topographic decay into the present. However, the nature of sediment transport in Coweeta may not be best constrained using Equation 1 as modeling work performed by Mudd (2016) suggests that a deviation of this magnitude

from the steady state curve indicates that a landscape is not undergoing pure nonlinear sediment flux.

440 6.2 Sensitivity analysis of averaging methods

Several of the techniques utilized to average the raw E^*R^* data have free parameters, the selection of which can influence the final results. In the following section we explore the influence of averaging technique, minimum patch and basin area, basin stream order and binning parameters can have on the interpretation of E^*R^* data.

445 6.2.1 Averaging methods

As outlined in Section 4.3 the topographic parameters, L_H , R , C_{HT} , and S_{HT} , must be smoothed in order to extract meaningful trends from the inherently noisy signal. The main technique for performing this smoothing is to spatially average the data over either hilltop patches or drainage basins. These averages can be computed as either the mean or the median of each spatial area. Figure 7
450 presents a comparison between hilltop patch data computed using means and medians for the Oregon Coast Range, showing little change between the measurements using the two techniques. As there is little difference between the two methods we use median values throughout this paper, as this ensures that any extreme values will have a lesser impact on landscape scale metrics.

6.2.2 Spatial averaging parameters

455 The hilltop patch identification process described in Section 3.1 requires one user defined parameter, the minimum patch area. This value is used to remove any small patches from the analysis and is included to ensure that patches conform to geomorphologically significant hillslopes, and not small patches of hilltop that are not representative of the hillslope as a whole. By varying the size of the minimum patch area from 0 through to 500 pixels it is possible to observe how this parameter can
460 impact the interpretation of E^*R^* data (Figure 8A). As the threshold is increased, fewer patches are considered valid and the density of the data ~~is~~are reduced, having the effect of removing many of the outlying data points. This reinforces the need to set a minimum size for a hilltop patch to ensure that a small number of measurements do not have too large an impact on the interpretation of the data.

465 The technique in Section 3.1 has no method to limit the maximum size of the hilltop patches, as the aim is to find spatially contiguous zones of hilltop and artificially breaking these patches may result in oversampling some sections of a landscape. Large patches make up a very small proportion of the total population of patches and correspondingly do not have a large impact on the overall trends in an individual dataset.

470 The number of valid data points contained within a basin used to generate an average value is another free parameter that the user must set. As with the hilltop patch area, selecting a sensible value

is important to ensure that each basin average data point corresponds to the basin as a whole and not just as a spatial subset. As the threshold is increased, outlying basins are removed (Figure 8B), indicating that many outlying data points are generated by a small number of irregular hillslopes in otherwise typical basins. However, if the threshold is too large, too many basins will be excluded. In order to ensure consistency between spatial averaging techniques it is recommended that the minimum number of pixels in a basin be kept equal with the minimum patch area.

The stream order of the basin used to generate basin average values will also have an influence on the interpretation of the results. [Grieve et al. \(2016\)](#) used second order basins to generate basin average topographic parameters as this order generated a large number of basins which all had a large enough area to generate numerous data points per basin effectively sampling as much of a landscape as possible. Figure 8C shows the effect of increasing the stream order of the basins used in Coweeta from first to fourth order. As each increasing order basin can be considered a set containing the previous order basins, the basin average points all plot in very similar locations in E^*R^* space, suggesting that increasing basin order may be a useful method of smoothing basin average data in noisy landscapes. However, this comes with the limitation that as the basin order increases, the number of basins in a landscape decreases, resulting in fewer data points representing larger spatial areas and the possible homogenization of topographic signals occurring at spatial scales smaller than the average basin area.

6.2.3 Log bin parameters

When computing logarithmically spaced bins there are two free parameters, number of bins, equivalent to the bin width and the minimum number of data points which must fall within a bin for the binned point to be valid. Figure 9A highlights the influence of changing the number of bins on the interpretation of the Cascade Ridge data. If the number of bins are too low, it becomes difficult to identify a trend in the data as the nature of a landscape can vary considerably across large ranges of E^* and by homogenizing these measurements a transient signal can be lost.

However, as the number of bins is increased, fewer values are placed into each bin resulting in a single value significantly different to the rest of the values in the bin, vastly altering the result. It is also the case that as the number of bins increases, the chance of a bin being removed for having too few data points increases, which will be particularly apparent at low and high E^* values, where the data is ~~is~~^{are} sparser. We have found that using 20 bins reaches a good compromise between data density and data smoothing, and corresponds well with the 21 bins used by Hurst et al. (2012), where no filtering was performed based on bin size.

The minimum size of each bin can also have an impact on the final interpretation of the data. If no threshold is applied, some bins can contain a single value, while others can contain hundreds of values which makes interpreting the data difficult as we cannot be sure of the robustness of each binned value. If the threshold is placed too high, then valid data will not be included in the final

analysis and the interpretation of a landscape's evolution could be incorrect. Figure 9B highlights this issue using data from Cascade Ridge at a range of bin size thresholds, identified as percentages of the total dataset size. We have found that using a minimum bin size of 1-5% of the total dataset ensures a good binning result.

6.3 Constraining S_c

Landscapes which are in topographic steady state should plot at a single location on the curve described by Equation 5. In principle this would mean that an erosion gradient would be required in order to constrain S_c , by fitting the data to the steady state curve. However, as observed in Figures 2 and 3 even in idealized steady state landscapes, there is still considerable variability in the E^*R^* data. This variability is consistent with patterns of dynamic reorganization of low order drainage basins within models of steady state landscapes performed by Reinhardt and Ellis (2015). Therefore it becomes possible to estimate the critical gradient of the nonlinear sediment flux law (Equation 1) for a landscape without a strong erosion gradient, using E^*R^* data.

As with previous analyses, the raw data must be spatially averaged in order to reduce the level of noise present in E^*R^* space before an estimate of S_c can be made. The optimal value of S_c is estimated using a nonlinear least squares method (Jones et al., 2001) which computes the sum of the square of the deviation between each measured E^*R^* value and the value predicted by Equation 5. This calculation is performed for a range of critical gradients until the S_c with the lowest corresponding deviation from the steady state curve is found.

The accuracy of this optimized S_c value is constrained ~~though~~ through bootstrapping the optimization procedure. The data are sampled with replacement to generate ~~100 thousand~~ 100 000 datasets, consisting of values randomly drawn from the population of patch or basin average data. For each of these sampled datasets the optimal value of S_c which minimizes the error between the data and the steady state curve is calculated. The final S_c value for each landscape is the mean value of these ~~100 thousand~~ 100 000 iterations, with a 95% confidence interval.

Table 1 contains estimates of the critical gradient generated using both basin and patch average values alongside previously published values for Cascade Ridge, the Oregon Coast Range and Gabilan Mesa. The predicted patch and basin average values for Gabilan Mesa and the Oregon Coast Range are similar to those published by ~~? and suggest that values proposed by Roering et al. (1999) are too large for these landscapes.~~ Grieve et al. (2016). This method of estimating the best fit S_c will produce an average value representative of the maximum probability density of S_c values for a landscape. Whereas the method of S_c estimation employed by Roering et al. (1999) can better be considered as the maximum S_c value for a landscape Grieve et al. (2016).

The data for Cascade Ridge shows better agreement with the value used by Hurst et al. (2012), which was also derived using E^*R^* data, than the lower estimate from ~~? Grieve et al. (2016)~~ Grieve et al. (2016). The pair of S_c values calculated for each landscape are very similar, suggesting that in large enough

datasets, the constraint of S_c is insensitive to the spatial scale of data averaging. However, the scale of spatial averaging has been demonstrated to have an impact on the interpretation of E^*R^* data and thus care must be taken to select appropriate methods of spatial averaging and data processing in order to ensure that results generated are not simply a function of user defined parameters.

The similarity of the average S_c values obtained using the bootstrapping procedure across three diverse landscapes highlights the presence of a distribution of E^*R^* values existing for each landscape, and the nature of an average S_c measurement. Such a distribution occurs due to local variations in topography, process and material properties and similarities can be drawn between the results presented in Table 1 and other similar studies (DiBiase et al., 2010; Hurst et al., 2012).

The values of S_c constrained using this bootstrapping procedure are similar to those derived from the relationship between hillslope length and relief demonstrated by Grieve et al. (2016), however there is no need to estimate material properties such as the soil and rock density and thus this method provides an independent constraint on S_c . However, the computational expense of bootstrapping the S_c fitting calculations from the E^*R^* data is very high, when contrasted with the estimation of S_c using $L_H - R$ relationships presented by Grieve et al. (2016). Additionally, using this bootstrapping method in landscapes which do not plot on the steady state curve in E^*R^* space can yield an incorrect S_c value with a low error estimate. Consequently, we recommend estimating the critical gradient of a landscape using this method and the method outlined in Grieve et al. (2016), when field data is available, in order to best constrain the critical gradient of a landscape. However, careful consideration of the differences between a maximum S_c and a best fit derived average S_c should be undertaken to ensure that a valid geomorphic interpretation of a landscape is employed.

7 Conclusions

We present a software package which automates the extraction and processing of high resolution topographic data to generate non-dimensional erosion rate and relief measurements. Topographic data can be averaged at a hilltop scale by generating unique hilltop patches or can be averaged over drainage basins automatically extracted from the channel network. Alongside the raw data, these spatially averaged datasets are shown to reproduce the findings of previous studies. In steady state landscapes such as the Oregon Coast Range and Gabilan Mesa E^*R^* data plots in a cluster around a single point on the steady state curve, supporting the conclusions drawn in previous studies (Roering et al., 2007); and in Cascade Ridge, a transient erosion signal similar to that identified by Hurst et al. (2012) is observed. This technique is also tested on a landscape in the Southern Appalachian mountains with the results suggesting that topography is decaying, supporting models of Miocene topographic rejuvenation proposed by Gallen et al. (2013). These compelling results, alongside the ability to reproduce previous work emphasizes the value of this software to the geomorphology com-

munity as until now, there has been no clear framework within which to produce non-dimensional erosion rate and relief measurements.

580 The average critical gradient used in Equation 1 is also constrained for three of the studied landscapes, with the values falling within expected ranges. However due to the noise inherent in this form of analysis and the challenges of evaluating the goodness of fit between such noisy data and a model, it is recommended that other methods to constrain S_c using the same raw data are utilized instead. Finally, the influence of free parameters on the final interpretation of the data ~~is~~are explored, 585 providing the user clear guidance on how to select parameters which control the level of smoothing or binning performed on the topographic data. The most significant of which are the minimum patch and basin size thresholds which must be carefully selected to balance smoothing the data with preserving landscape scale trends.

Author contributions.

590 SWDG developed the data analysis and visualization code and performed the data analysis. SWDG, SMM, MDH and DTM wrote the topographic analysis code. SWDG wrote the manuscript with contributions from SMM, MDH and DTM.

Acknowledgements. The topographic data used in this paper is freely available from <http://www.opentopography.org>. All the code used in this analysis is open source and can be downloaded from <https://github.com/LSDtopotools/> LSDTT_Hillslope_Analysis, http://github.com/sgrieve/ER_Star/ and http://github.com/sgrieve/ER_Star_Figs/. 595 The data used to generate all the plots are available from http://www.geos.ed.ac.uk/~s0675405/ER_Data/ER_Data.zip. SWDG is supported by NERC grant NE/J009970/1. SMM is supported by U.S. Army Research Office contract number W911NF-13-1-0478. DTM is supported by NERC grants NE/152830X/1 and J500021/1, in addition to the Harkness Award from the University of Cambridge. This paper is published with the permission 600 of the Executive Director of the British Geological Survey and was supported in part by the Climate and Landscape Change research programme at the BGS. We thank Fiona Clubb for discussions and advice which have shaped the final form of this manuscript.

Appendix A: Topographic Metadata

This table provides the accuracy information for the four point clouds used to generate the 1 meter 605 resolution topographic data used in this study. This information is compiled from metadata available from OpenTopography.org.

Table A1. LiDAR point cloud metadata.

Location	Point density (points per m^2)	Vertical accuracy (m)	Horizontal accuracy (m)
Oregon Coast Range	6.55	0.07 ± 0.03	0.06
Gabilan Mesa	5.56	0.20 ± 0.15	0.11
Cascade Ridge	9.84	0.17 ± 0.13	0.11
Coweeta	8.91	0.17 ± 0.13	0.11

References

- Anders, A. M., Roe, G. H., Montgomery, D. R., and Hallet, B.: Influence of precipitation phase on the form of mountain ranges, *Geology*, 36, 479–482, doi:10.1130/G24821A.1, <http://geology.gsapubs.org/content/36/6/479>, 2008.
- Andrews, D. J. and Bucknam, R. C.: Fitting degradation of shoreline scarps by a nonlinear diffusion model, *Journal of Geophysical Research: Solid Earth*, 92, 12 857–12 867, doi:10.1029/JB092iB12p12857, <http://onlinelibrary.wiley.com/doi/10.1029/JB092iB12p12857/abstract>, 1987.
- Baldwin, J. A., Whipple, K. X., and Tucker, G. E.: Implications of the shear stress river incision model for the timescale of postorogenic decay of topography, *Journal of Geophysical Research: Solid Earth*, 108, 2158, doi:10.1029/2001JB000550, <http://onlinelibrary.wiley.com/doi/10.1029/2001JB000550/abstract>, 2003.
- Benda, L. and Dunne, T.: Stochastic forcing of sediment supply to channel networks from landsliding and debris flow, *Water Resources Research*, 33, 2849–2863, https://www.wou.edu/las/physci/taylor/andrews_forest/refs/benda_dunne_1997.pdf, 1997.
- Binnie, S. A., Phillips, W. M., Summerfield, M. A., and Fifield, L. K.: Tectonic uplift, threshold hillslopes, and denudation rates in a developing mountain range, *Geology*, 35, 743–746, doi:10.1130/G23641A.1, <http://geology.gsapubs.org/content/35/8/743>, 2007.
- Booth, A. M., Roering, J. J., and Rempel, A. W.: Topographic signatures and a general transport law for deep-seated landslides in a landscape evolution model, *Journal of Geophysical Research: Earth Surface*, 118, 603–624, doi:10.1002/jgrf.20051, <http://onlinelibrary.wiley.com/doi/10.1002/jgrf.20051/abstract>, 2013.
- Braun, J., Heimsath, A. M., and Chappell, J.: Sediment transport mechanisms on soil-mantled hillslopes, *Geology*, 29, 683–686, doi:10.1130/0091-7613(2001)029<0683:STMOSM>2.0.CO;2, <http://geology.gsapubs.org/content/29/8/683>, 2001.
- Champagnac, J.-D., Molnar, P., Sue, C., and Herman, F.: Tectonics, climate, and mountain topography, *Journal of Geophysical Research: Solid Earth*, 117, B02 403, doi:10.1029/2011JB008348, <http://onlinelibrary.wiley.com.ezproxy.is.ed.ac.uk/doi/10.1029/2011JB008348/abstract>, 2012.
- Clarke, B. A. and Burbank, D. W.: Bedrock fracturing, threshold hillslopes, and limits to the magnitude of bedrock landslides, *Earth and Planetary Science Letters*, 297, 577–586, doi:10.1016/j.epsl.2010.07.011, <http://www.sciencedirect.com/science/article/pii/S0012821X10004498>, 2010.
- Clarke, B. A. and Burbank, D. W.: Quantifying bedrock-fracture patterns within the shallow subsurface: Implications for rock mass strength, bedrock landslides, and erodibility, *Journal of Geophysical*

Research: Earth Surface, 116, F04009, doi:10.1029/2011JF001987, <http://onlinelibrary.wiley.com/doi/10.1029/2011JF001987/abstract>, 2011.

Clubb, F. J., Mudd, S. M., Milodowski, D. T., Hurst, M. D., and Slater, L. J.: Objective extraction
640 of channel heads from high-resolution topographic data, *Water Resources Research*, 50, 4283–4304,
doi:10.1002/2013WR015167, <http://onlinelibrary.wiley.com/doi/10.1002/2013WR015167/abstract>, 2014.

Culling, W. E. H.: Analytical Theory of Erosion, *The Journal of Geology*, 68, 336–344, <http://www.jstor.org/stable/30059222>, 1960.

DiBiase, R. A., Whipple, K. X., Heimsath, A. M., and Ouimet, W. B.: Landscape form and millennial
645 erosion rates in the San Gabriel Mountains, CA, *Earth and Planetary Science Letters*, 289, 134–144,
doi:10.1016/j.epsl.2009.10.036, <http://www.sciencedirect.com/science/article/pii/S0012821X09006451>,
2010.

DiBiase, R. A., Heimsath, A. M., and Whipple, K. X.: Hillslope response to tectonic forcing in threshold
landscapes, *Earth Surface Processes and Landforms*, 37, 855–865, doi:10.1002/esp.3205, <http://onlinelibrary.wiley.com/doi/10.1002/esp.3205/abstract>, 2012.

Dietrich, W. E., Bellugi, D. G., Sklar, L. S., Stock, J. D., Heimsath, A. M., and Roering, J. J.: Geomorphic
Transport Laws for Predicting Landscape form and Dynamics, in: *Prediction in Geomorphology*, edited by
Wilcock, P. R. and Iverson, R. M., pp. 103–132, American Geophysical Union, Washington, D.C., <http://onlinelibrary.wiley.com/doi/10.1029/135GM09/summary>, 2003.

655 Dillencourt, M. B., Samet, H., and Tamminen, M.: A General Approach to Connected-component Labeling for
Arbitrary Image Representations, *J. ACM*, 39, 253–280, doi:10.1145/128749.128750, <http://doi.acm.org/10.1145/128749.128750>, 1992.

Dohrenwend, J. C.: Systematic valley asymmetry in the central California Coast Ranges, *Geological Society of America Bulletin*, 89, 891–900, doi:10.1130/0016-7606(1978)89<891:SVAITC>2.0.CO;2, <http://gsabulletin.gsapubs.org/content/89/6/891>, 1978.

Dohrenwend, J. C.: Morphologic Analysis of Gabilan Mesa by Iterative Contour-Generalization: An Improved
Method of Geomorphic Cartographic Analysis, *SEPM Pacific Coast Paleogeography Field Guide #4*, Menlo
Park, California, pp. 83–87, http://archives.datapages.com/data/pac_sepm/025/025001/pdfs/83.htm, 1979.

Foufoula-Georgiou, E., Ganti, V., and Dietrich, W. E.: A nonlocal theory of sediment transport on hill-
665 slopes, *Journal of Geophysical Research: Earth Surface*, 115, F00A16, doi:10.1029/2009JF001280, <http://onlinelibrary.wiley.com/doi/10.1029/2009JF001280/abstract>, 2010.

Furbish, D. J. and Fagherazzi, S.: Stability of creeping soil and implications for hillslope evolution, *Water Resources Research*, 37, 2607–2618, doi:10.1029/2001WR000239, <http://onlinelibrary.wiley.com/doi/10.1029/2001WR000239/abstract>, 2001.

670 Furbish, D. J. and Roering, J. J.: Sediment disentrainment and the concept of local versus nonlocal transport
on hillslopes, *Journal of Geophysical Research: Earth Surface*, 118, 937–952, doi:10.1002/jgrf.20071, <http://onlinelibrary.wiley.com/doi/10.1002/jgrf.20071/abstract>, 2013.

Gabet, E. J., Pratt-Sitaula, B. A., and Burbank, D. W.: Climatic controls on hillslope angle and relief in the Himalayas, *Geology*, 32, 629–632, doi:10.1130/G20641.1, <http://geology.gsapubs.org/content/32/7/629>, 2004.

675 Gabet, E. J., Mudd, S. M., Milodowski, D. T., Yoo, K., Hurst, M. D., and Dosseto, A.: Local topography and erosion rate control regolith thickness along a ridgeline in the Sierra Nevada, California, *Earth Surface Processes*

and Landforms, pp. 1779–1790, doi:10.1002/esp.3754, <http://onlinelibrary.wiley.com/doi/10.1002/esp.3754/abstract>, 2015.

Gallen, S. F., Wegmann, K. W., Frankel, K. L., Hughes, S., Lewis, R. Q., Lyons, N., Paris, P., Ross, K., Bauer, J. B., and Witt, A. C.: Hillslope response to knickpoint migration in the Southern Appalachians: implications for the evolution of post-orogenic landscapes, *Earth Surface Processes and Landforms*, 36, 1254–1267, doi:10.1002/esp.2150, <http://onlinelibrary.wiley.com/doi/10.1002/esp.2150/abstract>, 2011.

Gallen, S. F., Wegmann, K. W., and Bohnenstieh, D. R.: Miocene rejuvenation of topographic relief in the southern Appalachians, *GSA Today*, 23, 4–10, doi:10.1130/GSATG163A.1, <http://www.geosociety.org/gsatoday/archive/23/2/abstract/i1052-5173-23-2-4.htm>, 2013.

Grieve, S. W., Mudd, S. M., and Hurst, M. D.: How long is a hillslope?, *Earth Surface Processes and Landforms*, doi:10.1002/esp.3884, <http://onlinelibrary.wiley.com/doi/10.1002/esp.3884/abstract>, 2016.

Hales, T. C., Ford, C. R., Hwang, T., Vose, J. M., and Band, L. E.: Topographic and ecologic controls on root reinforcement, *Journal of Geophysical Research: Earth Surface*, 114, F03 013, doi:10.1029/2008JF001168, <http://onlinelibrary.wiley.com/doi/10.1029/2008JF001168/abstract>, 2009.

Hales, T. C., Scharer, K. M., and Wooten, R. M.: Southern Appalachian hillslope erosion rates measured by soil and detrital radiocarbon in hollows, *Geomorphology*, 138, 121–129, doi:10.1016/j.geomorph.2011.08.030, <http://www.sciencedirect.com/science/article/pii/S0169555X11004612>, 2012.

Hancock, G. R. and Evans, K. G.: Channel head location and characteristics using digital elevation models, *Earth Surface Processes and Landforms*, 31, 809–824, doi:10.1002/esp.1285, <http://onlinelibrary.wiley.com/doi/10.1002/esp.1285/abstract>, 2006.

He, L., Chao, Y., and Suzuki, K.: A Run-Based Two-Scan Labeling Algorithm, *IEEE Transactions on Image Processing*, 17, 749–756, doi:10.1109/TIP.2008.919369, 2008.

He, L.-F., Chao, Y.-Y., and Suzuki, K.: An Algorithm for Connected-Component Labeling, Hole Labeling and Euler Number Computing, *Journal of Computer Science and Technology*, 28, 468–478, doi:10.1007/s11390-013-1348-y, <http://link.springer.com/article/10.1007/s11390-013-1348-y>, 2013.

Heimsath, A. M., Dietrich, W. E., Nishiizumi, K., and Finkel, R. C.: Stochastic processes of soil production and transport: erosion rates, topographic variation and cosmogenic nuclides in the Oregon Coast Range, *Earth Surface Processes and Landforms*, 26, 531–552, doi:10.1002/esp.209, <http://onlinelibrary.wiley.com/doi/10.1002/esp.209/abstract>, 2001.

Heimsath, A. M., Furbish, D. J., and Dietrich, W. E.: The illusion of diffusion: Field evidence for depth-dependent sediment transport, *Geology*, 33, 949–952, doi:10.1130/G21868.1, <http://geology.gsapubs.org/content/33/12/949>, 2005.

Hilley, G. E. and Arrowsmith, J. R.: Geomorphic response to uplift along the Dragon’s Back pressure ridge, Carrizo Plain, California, *Geology*, 36, 367–370, doi:10.1130/G24517A.1, <http://geology.gsapubs.org/content/36/5/367>, 2008.

Hurst, M. D., Mudd, S. M., Walcott, R., Attal, M., and Yoo, K.: Using hilltop curvature to derive the spatial distribution of erosion rates, *Journal of Geophysical Research: Earth Surface*, 117, F02 017, doi:10.1029/2011JF002057, <http://onlinelibrary.wiley.com/doi/10.1029/2011JF002057/abstract>, 2012.

- 715 Hurst, M. D., Mudd, S. M., Attal, M., and Hilley, G.: Hillslopes Record the Growth and Decay of Landscapes, *Science*, 341, 868–871, doi:10.1126/science.1241791, <http://www.sciencemag.org/content/341/6148/868>, 2013a.
- Hurst, M. D., Mudd, S. M., Yoo, K., Attal, M., and Walcott, R.: Influence of lithology on hillslope morphology and response to tectonic forcing in the northern Sierra Nevada of California, *Journal of Geophysical Research: Earth Surface*, 118, 832–851, doi:10.1002/jgrf.20049, <http://onlinelibrary.wiley.com/doi/10.1002/jgrf.20049/abstract>, 2013b.
- 720 Jackson, M. and Roering, J. J.: Post-fire geomorphic response in steep, forested landscapes: Oregon Coast Range, USA, *Quaternary Science Reviews*, 28, 1131–1146, doi:10.1016/j.quascirev.2008.05.003, <http://adsabs.harvard.edu/abs/2009QSRv...28.1131J>, 2009.
- 725 Jones, E., Oliphant, T., and Peterson, P.: SciPy: Open source scientific tools for Python, <http://www.scipy.org/>, [Online; accessed 2015-08-03], 2001.
- Kelsey, H. M., Ticknor, R. L., Bockheim, J. G., and Mitchell, E.: Quaternary upper plate deformation in coastal Oregon, *Geological Society of America Bulletin*, 108, 843–860, doi:10.1130/0016-7606(1996)108<0843:QUPDIC>2.3.CO;2, <http://gsabulletin.gsapubs.org/content/108/7/843>, 1996.
- 730 Kim, H., Arrowsmith, J., Crosby, C. J., Jaeger-Frank, E., Nandigam, V., Memon, A., Conner, J., Baden, S. B., and Baru, C.: An efficient implementation of a local binning algorithm for digital elevation model generation of LiDAR/ALSM dataset, in: *AGU Fall Meeting Abstracts*, vol. 1, p. 0921, San Francisco, <http://adsabs.harvard.edu/abs/2006AGUFM.G53C0921K>, 2006.
- Korup, O.: Rock type leaves topographic signature in landslide-dominated mountain ranges, *Geophysical Research Letters*, 35, L11402, doi:10.1029/2008GL034157, <http://onlinelibrary.wiley.com/doi/10.1029/2008GL034157/abstract>, 2008.
- 735 Lashermes, B., Foufoula-Georgiou, E., and Dietrich, W. E.: Channel network extraction from high resolution topography using wavelets, *Geophysical Research Letters*, 34, L23S04, doi:10.1029/2007GL031140, <http://onlinelibrary.wiley.com/doi/10.1029/2007GL031140/abstract>, 2007.
- 740 Lumia, R., Shapiro, L., and Zuniga, O.: A new connected components algorithm for virtual memory computers, *Computer Vision, Graphics, and Image Processing*, 22, 287–300, doi:10.1016/0734-189X(83)90071-3, <http://www.sciencedirect.com/science/article/pii/0734189X83900713>, 1983.
- Matmon, A., Bierman, P. R., Larsen, J., Southworth, S., Pavich, M., and Caffee, M.: Temporally and spatially uniform rates of erosion in the southern Appalachian Great Smoky Mountains, *Geology*, 31, 155–158, doi:10.1130/0091-7613(2003)031<0155:TASURO>2.0.CO;2, <http://geology.gsapubs.org/content/31/2/155>, 2003.
- 745 McKean, J. A., Dietrich, W. E., Finkel, R. C., Southon, J. R., and Caffee, M. W.: Quantification of soil production and downslope creep rates from cosmogenic ^{10}Be accumulations on a hillslope profile, *Geology*, 21, 343–346, doi:10.1130/0091-7613(1993)021<0343:QOSPAD>2.3.CO;2, <http://geology.gsapubs.org/content/21/4/343>, 1993.
- 750 Milodowski, D. T., Mudd, S. M., and Mitchard, E. T.: Erosion rates as a potential bottom-up control of forest structural characteristics in the Sierra Nevada Mountains, *Ecology*, 96, 31–38, <http://www.esajournals.org/doi/abs/10.1890/14-0649.1>, 2015a.

- Milodowski, D. T., Mudd, S. M., and Mitchard, E. T. A.: Topographic roughness as a signature of the emergence
755 of bedrock in eroding landscapes, doi:10.5194/esurf-3-483-2015, <http://www.earth-surf-dynam.net/3/483/2015/>, 2015b.
- Montgomery, D. R. and Foufoula-Georgiou, E.: Channel network source representation using digital elevation models, *Water Resources Research*, 29, 3925–3934, doi:10.1029/93WR02463, <http://onlinelibrary.wiley.com/doi/10.1029/93WR02463/abstract>, 1993.
- 760 Montgomery, D. R., Sullivan, K., and Greenberg, H. M.: Regional test of a model for shallow landsliding, *Hydrological Processes*, 12, 943–955, <http://rocky.ess.washington.edu/grg/publications/pdfs/hyd-proc-v12-1998.pdf>, 1998.
- Mudd, S. M.: Detection of transience in eroding landscapes, *Earth Surface Processes and Landforms*, 2016.
- Mudd, S. M. and Furbish, D. J.: Influence of chemical denudation on hillslope morphology, *Journal of Geophysical Research: Earth Surface*, 109, F02 001, doi:10.1029/2003JF000087, <http://onlinelibrary.wiley.com/doi/10.1029/2003JF000087/abstract>, 2004.
- 765 Orlandini, S., Tarolli, P., Moretti, G., and Dalla Fontana, G.: On the prediction of channel heads in a complex alpine terrain using gridded elevation data, *Water Resources Research*, 47, W02 538, doi:10.1029/2010WR009648, <http://onlinelibrary.wiley.com/doi/10.1029/2010WR009648/abstract>, 2011.
- 770 Passalacqua, P., Do Trung, T., Foufoula-Georgiou, E., Sapiro, G., and Dietrich, W. E.: A geometric framework for channel network extraction from lidar: Nonlinear diffusion and geodesic paths, *Journal of Geophysical Research: Earth Surface*, 115, F01 002, doi:10.1029/2009JF001254, <http://onlinelibrary.wiley.com/doi/10.1029/2009JF001254/abstract>, 2010.
- Pelletier, J. D.: A robust, two-parameter method for the extraction of drainage networks from high-
775 resolution digital elevation models (DEMs): Evaluation using synthetic and real-world DEMs, *Water Resources Research*, 49, 75–89, doi:10.1029/2012WR012452, <http://onlinelibrary.wiley.com/doi/10.1029/2012WR012452/abstract>, 2013.
- Perron, J. T., Kirchner, J. W., and Dietrich, W. E.: Formation of evenly spaced ridges and valleys, *Nature*, 460, 502–505, doi:10.1038/nature08174, <http://www.nature.com/nature/journal/v460/n7254/abs/nature08174.html>, 2009.
- 780 Reinhardt, L. and Ellis, M. A.: The emergence of topographic steady state in a perpetually dynamic self-organized critical landscape, *Water Resources Research*, 51, 4986–5003, doi:10.1002/2014WR016223, <http://onlinelibrary.wiley.com/doi/10.1002/2014WR016223/abstract>, 2015.
- Reneau, S. L. and Dietrich, W. E.: Erosion rates in the southern oregon coast range: Evidence for an equilibrium between hillslope erosion and sediment yield, *Earth Surface Processes and Landforms*, 16, 307–322, doi:10.1002/esp.3290160405, <http://onlinelibrary.wiley.com/doi/10.1002/esp.3290160405/abstract>, 1991.
- 785 Riebe, C. S., Kirchner, J. W., Granger, D. E., and Finkel, R. C.: Erosional equilibrium and disequilibrium in the Sierra Nevada, inferred from cosmogenic ^{26}Al and ^{10}Be in alluvial sediment, *Geology*, 28, 803–806, doi:10.1130/0091-7613(2000)28<803:EEADIT>2.0.CO;2, <http://geology.gsapubs.org/content/28/9/803>, 2000.
- 790 Roering, J. J.: How well can hillslope evolution models “explain” topography? Simulating soil transport and production with high-resolution topographic data, *Geological Society of America Bulletin*, 120, 1248–1262, doi:10.1130/B26283.1, <http://gsabulletin.gsapubs.org/content/120/9-10/1248>, 2008.

Roering, J. J., Kirchner, J. W., and Dietrich, W. E.: Evidence for nonlinear, diffusive sediment transport on hillslopes and implications for landscape morphology, *Water Resources Research*, 35, 853–870, doi:10.1029/1998WR900090, <http://onlinelibrary.wiley.com/doi/10.1029/1998WR900090/abstract>, 1999.

Roering, J. J., Kirchner, J. W., and Dietrich, W. E.: Hillslope evolution by nonlinear, slope-dependent transport: Steady state morphology and equilibrium adjustment timescales, *Journal of Geophysical Research: Solid Earth*, 106, 16 499–16 513, doi:10.1029/2001JB000323, <http://onlinelibrary.wiley.com/doi/10.1029/2001JB000323/abstract>, 2001.

Roering, J. J., Perron, J. T., and Kirchner, J. W.: Functional relationships between denudation and hillslope form and relief, *Earth and Planetary Science Letters*, 264, 245–258, doi:10.1016/j.epsl.2007.09.035, <http://www.sciencedirect.com/science/article/pii/S0012821X07006061>, 2007.

Roering, J. J., Marshall, J., Booth, A. M., Mort, M., and Jin, Q.: Evidence for biotic controls on topography and soil production, *Earth and Planetary Science Letters*, 298, 183–190, doi:10.1016/j.epsl.2010.07.040, <http://www.sciencedirect.com/science/article/pii/S0012821X10004784>, 2010.

Rosenbloom, N. A. and Anderson, R. S.: Hillslope and channel evolution in a marine terraced landscape, Santa Cruz, California, *Journal of Geophysical Research: Solid Earth*, 99, 14 013–14 029, doi:10.1029/94JB00048, <http://onlinelibrary.wiley.com/doi/10.1029/94JB00048/abstract>, 1994.

Rosenfeld, A. and Pfaltz, J. L.: Sequential operations in digital picture processing, *Journal of the ACM (JACM)*, 13, 471–494, <http://dl.acm.org/citation.cfm?id=321357>, 1966.

Samet, H.: Connected Component Labeling Using Quadrees, *J. ACM*, 28, 487–501, doi:10.1145/322261.322267, <http://doi.acm.org/10.1145/322261.322267>, 1981.

Schmidt, K. M., Roering, J. J., Stock, J. D., Dietrich, W. E., Montgomery, D. R., and Schaub, T.: The variability of root cohesion as an influence on shallow landslide susceptibility in the Oregon Coast Range, *Canadian Geotechnical Journal*, 38, 995–1024, doi:10.1139/t01-031, <http://www.nrcresearchpress.com/doi/abs/10.1139/t01-031>, 2001.

Shreve, F.: The Vegetation of a Coastal Mountain Range, *Ecology*, 8, 27–44, doi:10.2307/1929384, <http://www.jstor.org/stable/1929384>, 1927.

Small, E. E., Anderson, R. S., and Hancock, G. S.: Estimates of the rate of regolith production using ¹⁰Be and ²⁶Al from an alpine hillslope, *Geomorphology*, 27, 131–150, doi:10.1016/S0169-555X(98)00094-4, <http://www.sciencedirect.com/science/article/pii/S0169555X98000944>, 1999.

Sofia, G., Pirotti, F., and Tarolli, P.: Variations in multiscale curvature distribution and signatures of LiDAR DTM errors, *Earth Surface Processes and Landforms*, 38, 1116–1134, doi:10.1002/esp.3363, <http://onlinelibrary.wiley.com/doi/10.1002/esp.3363/abstract>, 2013.

Stock, G. M., Anderson, R. S., and Finkel, R. C.: Pace of landscape evolution in the Sierra Nevada, California, revealed by cosmogenic dating of cave sediments, *Geology*, 32, 193–196, doi:10.1130/G20197.1, <http://geology.gsapubs.org/content/32/3/193>, 2004.

Stock, J. and Dietrich, W. E.: Valley incision by debris flows: Evidence of a topographic signature, *Water Resources Research*, 39, 1089, doi:10.1029/2001WR001057, <http://onlinelibrary.wiley.com/doi/10.1029/2001WR001057/abstract>, 2003.

- Suzuki, K., Horiba, I., and Sugie, N.: Linear-time connected-component labeling based on sequential local operations, *Computer Vision and Image Understanding*, 89, 1–23, doi:10.1016/S1077-3142(02)00030-9, <http://www.sciencedirect.com/science/article/pii/S1077314202000309>, 2003.
- 835 Sweeney, K. E., Roering, J. J., and Ellis, C.: Experimental evidence for hillslope control of landscape scale, *Science*, 349, 51–53, doi:10.1126/science.aab0017, <http://www.sciencemag.org/content/349/6243/51>, 2015.
- Swift Jr., L. W., Cunningham, G. B., and Douglass, J. E.: Climatology and Hydrology, in: *Forest Hydrology and Ecology at Coweeta*, edited by Swank, W. T. and Jr, D. A. C., no. 66 in *Ecological Studies*, pp. 35–55, Springer New York, http://link.springer.com/chapter/10.1007/978-1-4612-3732-7_3, 1988.
- 840 Tarolli, P.: High-resolution topography for understanding Earth surface processes: Opportunities and challenges, *Geomorphology*, 216, 295–312, doi:10.1016/j.geomorph.2014.03.008, <http://www.sciencedirect.com/science/article/pii/S0169555X14001202>, 2014.
- Tarolli, P. and Dalla Fontana, G.: Hillslope-to-valley transition morphology: New opportunities from high resolution DTMs, *Geomorphology*, 113, 47–56, doi:10.1016/j.geomorph.2009.02.006, <http://www.sciencedirect.com/science/article/pii/S0169555X09000646>, 2009.
- 845 Tseng, C.-M., Lin, C.-W., Dalla Fontana, G., and Tarolli, P.: The topographic signature of a major typhoon, *Earth Surface Processes and Landforms*, 40, 1129–1136, doi:10.1002/esp.3708, <http://onlinelibrary.wiley.com/doi/10.1002/esp.3708/abstract>, 2015.
- Tucker, G. E. and Bradley, D. N.: Trouble with diffusion: Reassessing hillslope erosion laws with a particle-based model, *Journal of Geophysical Research: Earth Surface*, 115, F00A10, doi:10.1029/2009JF001264, <http://onlinelibrary.wiley.com/doi/10.1029/2009JF001264/abstract>, 2010.
- 850 Tucker, G. E. and Slingerland, R.: Drainage basin responses to climate change, *Water Resources Research*, 33, 2031–2047, doi:10.1029/97WR00409, <http://onlinelibrary.wiley.com/doi/10.1029/97WR00409/abstract>, 1997.
- 855 Tucker, G. E., Catani, F., Rinaldo, A., and Bras, R. L.: Statistical analysis of drainage density from digital terrain data, *Geomorphology*, 36, 187–202, doi:10.1016/S0169-555X(00)00056-8, <http://www.sciencedirect.com/science/article/pii/S0169555X00000568>, 2001.
- Wiener, N.: *Extrapolation, interpolation, and smoothing of stationary time series*, vol. 2, MIT press Cambridge, MA, <http://tocs.ulb.tu-darmstadt.de/129776289.pdf>, 1949.
- 860 Wobus, C., Whipple, K. X., Kirby, E., Snyder, N., Johnson, J., Spyropolou, K., Crosby, B., and Sheehan, D.: Tectonics from topography: Procedures, promise, and pitfalls, *Geological Society of America Special Papers*, 398, 55–74, doi:10.1130/2006.2398(04), <http://specialpapers.gsapubs.org/content/398/55>, 2006.

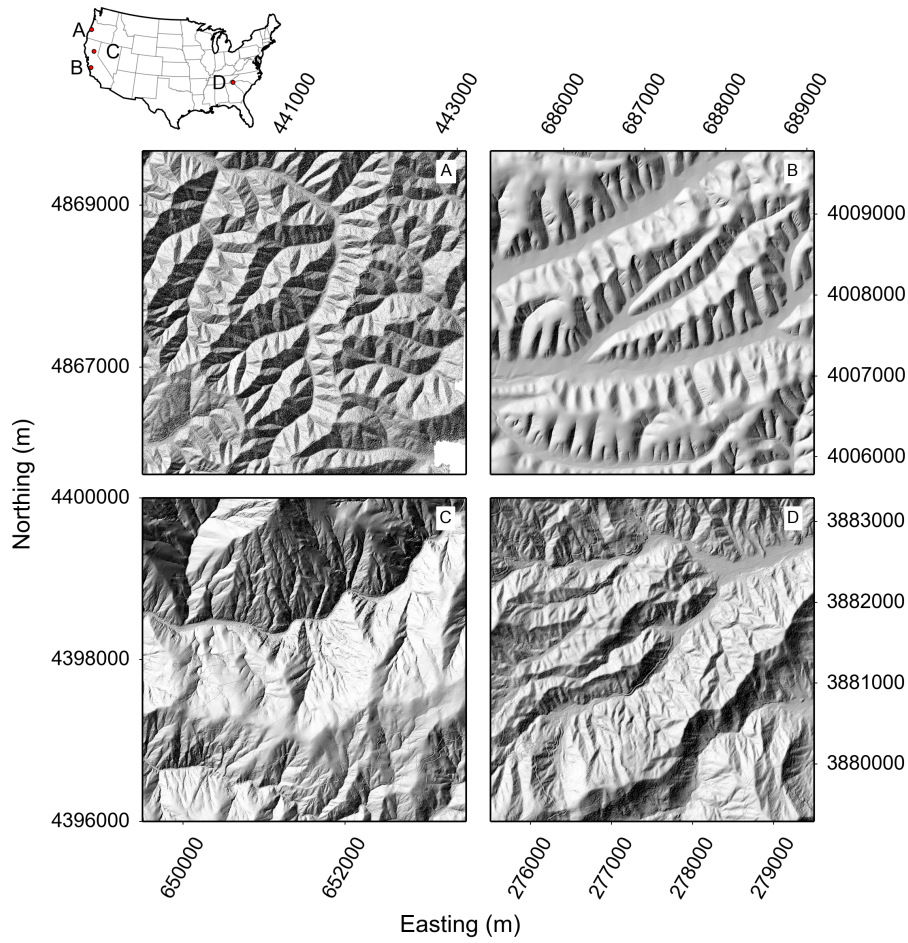


Figure 1. Map of the locations of each field site within the continental USA with a shaded relief map of characteristic sections of each location's topography. All coordinates are in UTM. (A) Oregon Coast Range, Oregon, UTM Zone 10N. (B) Gabilan Mesa, California, UTM Zone 10N. (C) Northern Sierra Nevada, California, UTM Zone 10N. (D) Coweeta, North Carolina, UTM Zone 17N.

Table 1. Previously published S_c values alongside the values generated from the best fit to the steady state curve for the patch and basin average data.

	Roering et al. (2007)	Hurst et al. (2012)	Grieve et al. (2016)	Patch Average ¹	Basin Average ²
Oregon Coast Range	1.2 ± 0.2	—	0.79	0.83 ± 0.01	0.83 ± 0.01
Gabilan Mesa	1.2 ± 0.4	—	0.8	$0.8^{+0.06}_{-0.05}$	$0.8^{+0.05}_{-0.04}$
Cascade Ridge	—	0.8	0.72	0.78 ± 0.02	0.82 ± 0.02

¹ Calculated as the value which minimizes the sum of the squared residuals to the steady state line for the patch average data. Error is the 95% confidence interval generated by bootstrapping the calculation 100 000 times.

² As for ¹ but using basin average data.

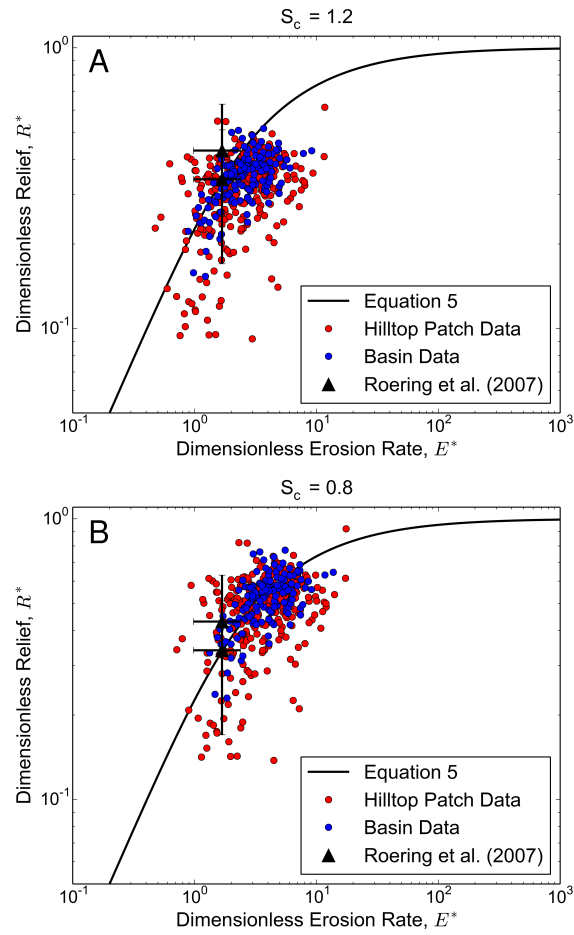


Figure 2. Hilltop patch and basin average data for Gabilan Mesa plotted using a critical gradient of 1.2 (A) and 0.8 (B) alongside data from Roering et al. (2007) for the same location. Errorbars are the standard error.

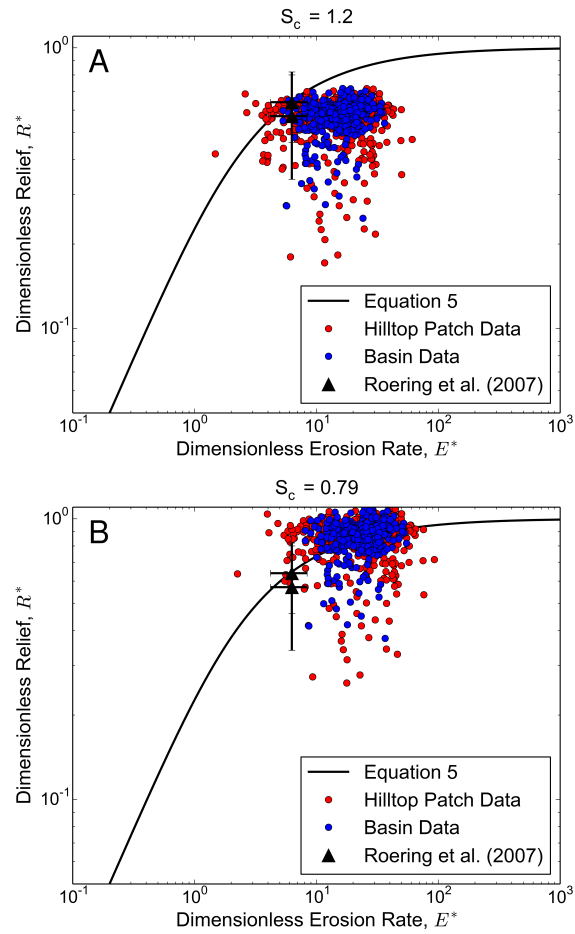


Figure 3. Hilltop patch and basin average data for the Oregon Coast Range plotted using a critical gradient of 1.2 (A) and 0.8 (B) alongside data from Roering et al. (2007) for the same location. Errorbars are the standard error.

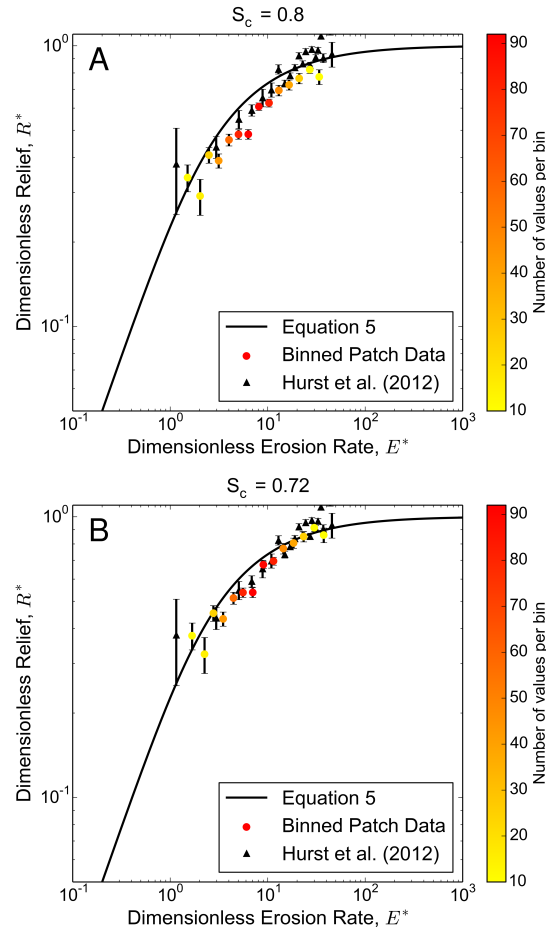


Figure 4. Binned hilltop patch data spanning a wide range of E^* values generated using a critical gradient of 0.8 (A) and 0.72 (B) alongside data from Hurst et al. (2012) for the same location. Errorbars are the standard error of the data. Errorbars from Hurst et al. (2012) are generated from the original data.

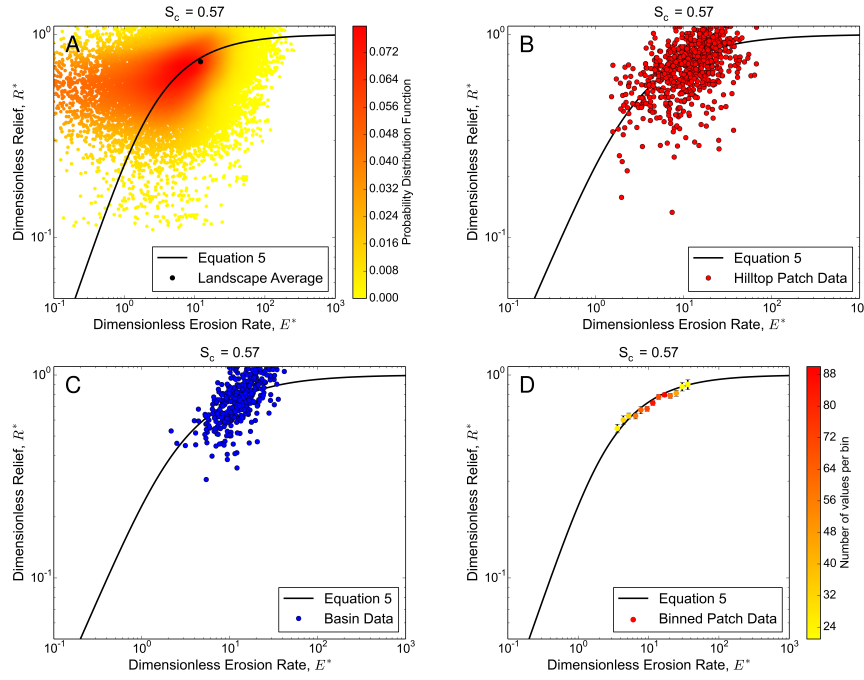


Figure 5. Comparison of the different methods which can be used to visualize $E^* R^*$ from Coweeta, using a critical gradient of 0.57. (A) Raw data colored by the density of points in $E^* R^*$ space alongside the landscape average value. Errorbars plot inside the data point. (B) Data averaged over hilltop patches. (C) Data averaged over second order drainage basins. (D) Hilltop patch data placed into logarithmically spaced bins, errorbars are the standard error.

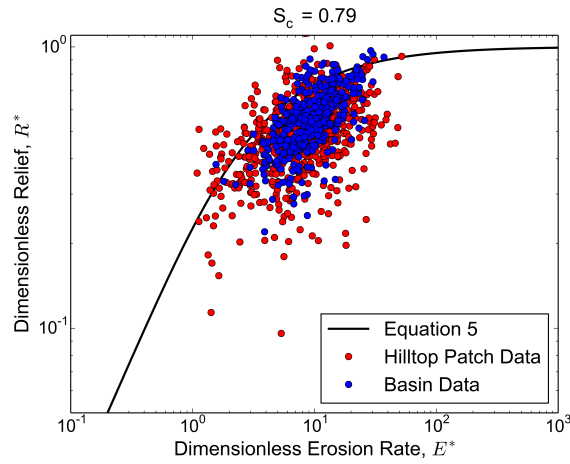


Figure 6. Hilltop patch data plotted using the higher S_c value of 0.79, demonstrating that the majority of the hillslopes in this landscape plot below the steady state curve when using a larger critical gradient.

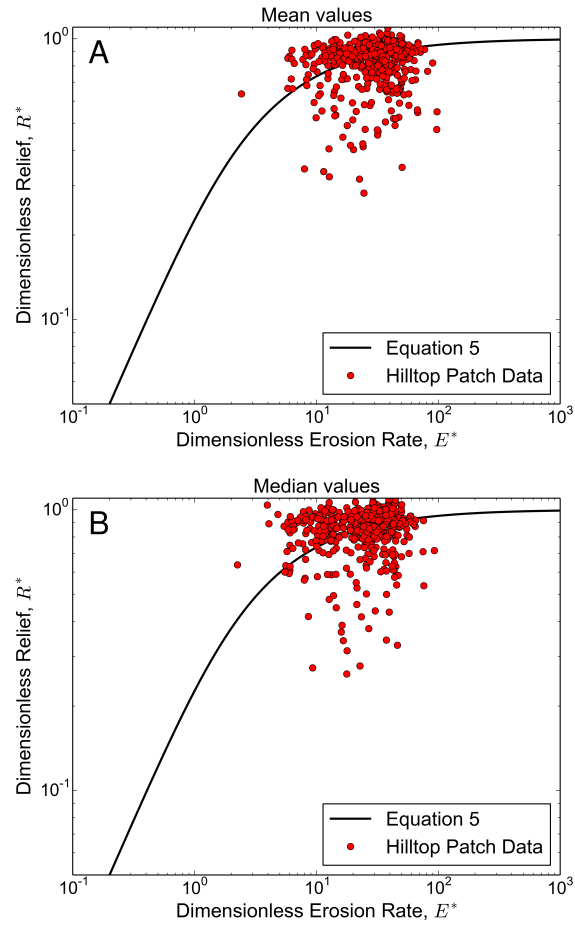


Figure 7. Comparison between hilltop patch values generated using a spatial mean (A) and a spatial median (B) for the Oregon Coast Range.

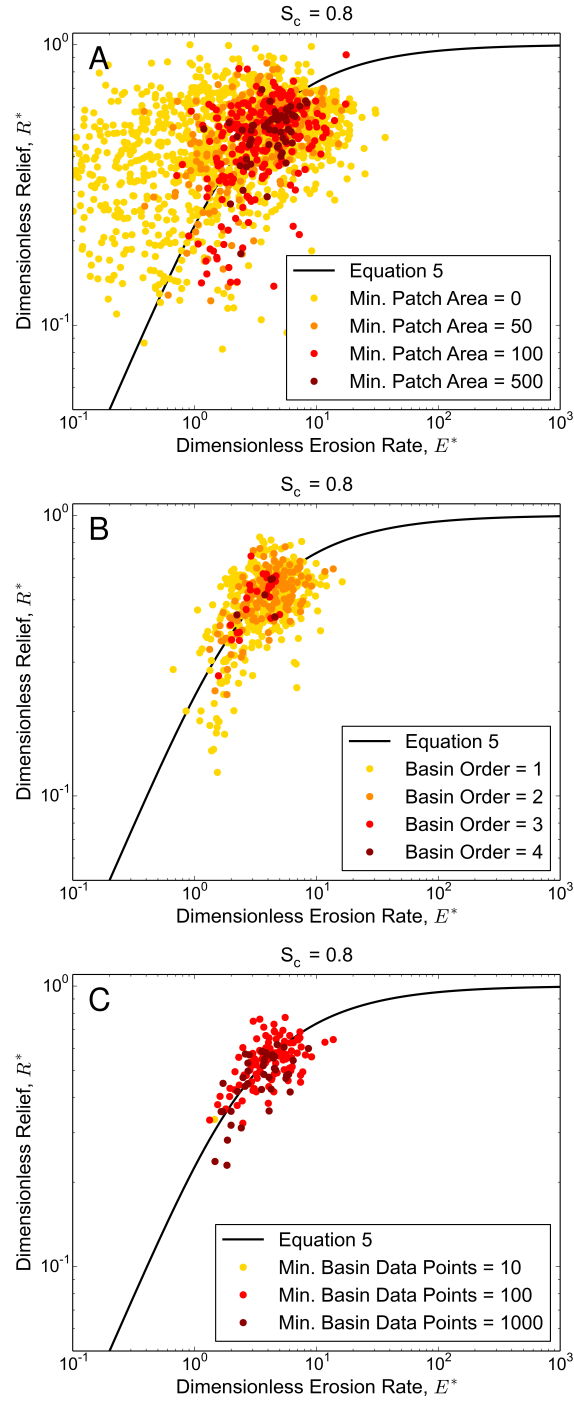


Figure 8. Comparison of the influence of changing spatial averaging method on the interpretation of E^*R^* data for Gabilan Mesa. (A) variations in the minimum patch area threshold from 0 (no threshold) to 500 pixels highlighting the reduction in noise when a minimum patch area is applied. (B) variations in the minimum basin pixels threshold. Outlying basins have very few data points, so are influenced more strongly by single atypical values. (C) increasing the basin stream order, which reduces variance in the data as bigger basins are sets containing basins of smaller orders, dampening any extreme values.

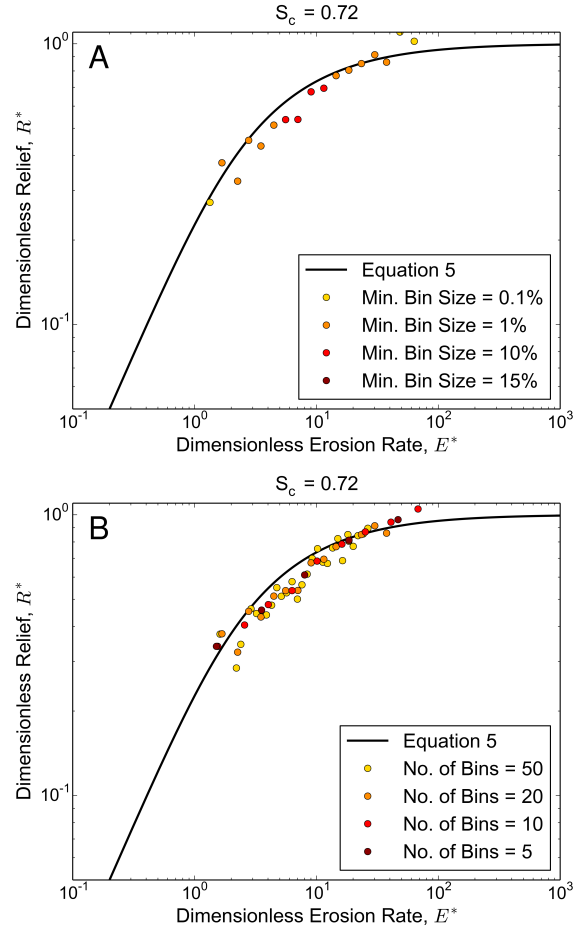


Figure 9. Comparison of the influence of binning parameters on the interpretation of E^*R^* data for Cascade Ridge. (A) varying the number of bins used, equivalent to the bin width in E^* space. As the number of bins reduces it becomes harder to identify patterns in the data and as the number of bins increases, the number of data points in each bin reduces, thereby reducing the power of the binning technique. (B) varying the minimum number of data points required in a basin. As this value increases fewer points are preserved, which compresses the range of the data and can obscure the observation of an erosional gradient. Too small a threshold can result in bins containing very few values which do not represent the landscape as a whole.